ISSN 0287-9808

KURRI-TR-444

京都大学臨界集合体実験装置における
加速器駆動システムの実験ベンチマーク

Experimental Benchmarks for Accelerator-Driven System (ADS) at

Kyoto University Critical Assembly

編集：卞　哲浩

Edited by Cheol Ho Pyeon

京都大学原子炉実験所

Research Reactor Institute, Kyoto University

Preface

These benchmark problems were contributed to the Coordinated Research Project (CRP) on "Analytical and Experimental Benchmark Analyses of Accelerator Driven Systems" in the International Atomic Energy Agency (IAEA), as entitled "**Experimental Benchmarks for Accelerator-Driven System (ADS) at the Kyoto University Critical Assembly (KUCA)**," from 2005 to 2009.

The major objective of these benchmarks is to contribute to research and development of ADS through the ADS experimental data with the use of 14 MeV neutrons carried out in the KUCA A-core.

These benchmarks are composed of these following items:

Phase I: Static experiments on ADS
Phase II: Kinetic Experiments on ADS

Special thanks are due KUCA staff and students for support and patience throughout a series of ADS experiments carried out at KUCA.

Cheol Ho Pyeon

December 2012

Keywords:
ADS, KUCA, A-core, Experiments, 14 MeV Neutrons

要　旨

この実験ベンチマーク問題は、国際原子力機関（IAEA）において 2005 年から 2009 年にかけて行われた共同研究プロジェクト「加速器駆動システムの実験解析」の一部として採択された「京都大学臨界集合体における加速器駆動システムの実験ベンチマーク」である。

この実験ベンチマーク問題は、KUCA の A 架台において行われた 14 MeV 中性子（パルス中性子発生装置）を用いた実験を通して ADS の研究開発に貢献することを目的としている。

この実験ベンチマーク問題は以下の項目から構成されている。

Phase I：静特性実験
Phase II：動特性実験

最後に、KUCA において ADS 実験を準備および運転にご協力をいただいた KUCA のスタッフ、実験における測定および数値解析に献身的に取り組んだ KUCA 棟に在籍していた学生諸君に心から感謝の意を表します。

卞　哲浩

2012 年 12 月

Contents

目　次

Experimental Benchmarks for Accelerator-Driven System (ADS) at Kyoto University Critical Assembly (KUCA)

Phase 1

Kyoto University Research Reactor Institute, Japan

Cheolho Pyeon

1. Experimental Benchmarks

1-1. Introduction

The accelerator-driven system (ADS) was developed for producing energy and for transmuting minor actinides and long-lived fission products. The ADSR has attracted worldwide attention in recent years because of its superior safety characteristics and potential for burning plutonium and nuclear waste. An outstanding advantage of its use is the anticipated absence of reactivity accidents, provided sufficient subcriticality is ensured. At the Kyoto University Research Reactor Institute (KURRI), a series of experiments for the ADSR was officially launched in fiscal 2000 at Kyoto University Critical Assembly (KUCA), with sights on a future plan (**K**umatori **A**ccelerator Driven **R**eactor **T**est Facility **&** Innovation Research **Labo**ratory: Kart & Lab. Project). A new accelerator will be attached to the KUCA facility in March 2008, and high-energy neutrons, generated by the interaction of high-energy proton beam 150MeV with heavy metal (Tungsten target), will be injected into KUCA in March 2008. The new accelerator is called the Fixed Field Alternating Gradient (FFAG) accelerator of the synchrotron type developed by High Energy Accelerator Research Organization (KEK) in Japan.

At KUCA, by combining a critical assembly of a solid-moderated and -reflected type core with a Cockcroft-Walton type accelerator, 14MeV pulsed neutrons generated by D-T (Deuteron – Tritium) reactions were injected through a polyethylene reflector into the subcritical system, where highly enriched uranium fuel was loaded together with the moderated polyethylene reflector. In these experiments, subcriticality is varied systematically by inserting control or safety rods, or both, into critical system. Presently, the neutron shield and the beam duct are installed in the reflector region for directing the high-energy neutrons generated in a tritium target to the fuel region, since the tritium target used by D-T reactions is located outside the core.

The main objectives of the present experiments are to examine experimentally the neutronic characteristics of the reaction rate distribution and the neutron spectrum of the ADSR at KUCA, to establish measurement techniques of neutronic parameters in the subcritical system and to investigate the accuracy of the neutronic design of the ADSR in its present state.

Analysts who execute calculations for some or all of these benchmarks are invited to contribute their results for eventual inclusion in this or a companion document. The specific information requested is identified in the appendix, along with an address to which that information may be sent.

1-2. Benchmark Specifications

1-2-1. Description of KUCA core

KUCA comprises solid-moderated and -reflected type-A and -B cores, and a water-moderated and -reflected type-C core. In the present series of experiments, the solid-moderated and -reflected type-A core was combined with a Cockcroft-Walton type pulsed neutron generator installed at KUCA.

The A-core (A3/8"P36EU(3)) configuration used for measuring the reaction rate distribution and the neutron spectrum is shown in Fig. 1-1. The fuel rods were constructed of a combination of 23 elements that were loaded on the grid plate. The materials used in the critical assemblies were always in the form of rectangular parallelepipe, normally 2" sq. with thickness ranging between 1/16" and 2". The upper and lower parts of the fuel region were polyethylene reflector layers of more than 50cm long, as shown in Fig. 1-2. The fuel rod, a 93% enriched Uranium-Aluminum (U-Al) alloy, consisted of 36 cells of 2 polyethylene plates 1/8" and 1/4" thick, and a U-Al plate 1/16" thick and 2" sq. The functional height of the core was approximately 40cm.

1-2-2. Description of 14MeV Pulsed neutron generator

The pulsed neutron generator was combined with the A-core, where 14MeV pulsed neutrons were injected into the subcritical system through the polyethylene reflector. In the experiments, the deuteron beam (accelerated up to 160keV in beam energy, 4.5mA in beam current, 10μs in pulse width and 500Hz in pulse repetition rate) was led to the tritium target located outside the polyethylene reflector. At the pulsed neutron generator, the beam peak intensity is about 0.5mA for a pulse width of up to 100μs, and the repetition rate varies from a few Hz to 30kHz, providing up to 1×10^8 n/s.

1-2-3. Installation of Neutron shield and Beam duct

The tritium target is not placed at the center of the core. In the experiments, therefore, the neutron shield and the beam duct were installed in the polyethylene reflector region shown in Fig. 1-1. The main purpose of installing the neutron shield and the beam duct was to direct the highest number possible of the high-energy neutrons generated in the target region to the center of the core.

For shielding the high-energy and thermal neutrons, the neutron shield comprises several materials inserted into the core, as shown in Figs. 1-12, 1-13 and 1-14: the iron (Fe) for shielding the high-energy neutrons generated in the target region by inelastic scattering reactions; the polyethylene containing 10wt% boron for shielding the thermal neutrons, moderated by absorption reactions, in the reflector region; the beam duct (void) for directing collimated high-energy neutrons, by streaming effect, to the core region.

1-3. Desired Results

1-3-1. Excess reactivity and Subcriticality

The critical state was adjusted by maintaining the control rods in certain positions, and the subcritical state was acquired by inserting the control or safety rods, or both, up to the lower limit in the critical state. The subcriticality was obtained from the combination of both the reactivity worth of each control rod evaluated by the rod drop method and the excess reactivity on the basis of its integral calibration curve obtained by the positive period method. For eigenvalue and source calculations, it is necessary to consider the activation foils themselves set in the position of (15, K) shown in Fig. 1-1. Note that the atomic density, the variation and the size of each foil are shown in Tables III-6, IV-2 and IV-3, respectively.

1-3-2. Indium (In) reaction rate distribution

Indium (In) wire 1.5mmϕ in diameter and 60cm long was set in the axial center position along (16,17–J,W) the vertical shown in Fig. 1-1, for measuring the reaction rate distribution. Refer to Fig. 1-10 in detail. The experimental results of the In wire were obtained by measuring total counts of the peak energy of γ-ray emittance and normalized by the counts of another irradiated In foil ($20\times20\times1$ mm^3) emitted from ^{115}In(n, n')^{115m}In reactions set in the location of the tritium target.

1-3-3. Reaction rates of activation foils

Activation foils were set in an objective positions, including (15, K) and tritium target shown in Fig. 1-1, for measuring the neutron spectrum. The size of the activation foils was 45mm$\times$45mm with thickness varying between 3 and 5mm. They were selected for covering as wide a range as possible of threshold energy values within 14MeV neutrons. The experimental results of the reaction rates of all the irradiated activation foils were obtained by measuring total counts of the peak energy of γ-ray emittance and normalized by the counts of another irradiated Nb foil ($50\times50\times1$ mm^3) emitted from ^{93}Nb(n, 2n)^{92m}Nb reactions set in the location of the tritium target. In measuring the neutron spectrum, the activation foils were set as an aggregate of several samples, and two sets (Foils No. 2 and 3 shown in Table IV-2) of the activation foils were irradiated simultaneously at the positions of interest (15, K) and the target, for obtaining neutron spectral information.

1-4. References

[1] S. Shiroya, H. Unesaki, Y. Kawase, H. Moriyama and M. Inoue, "Accelerator Driven Subcritical System as A Future Neutron Source in Kyoto University Research Reactor Institute (KURRI) – Basic Study on Neutron Multiplication in the Accelerator Driven Subcritical Reactor," *Prog. Nucl. Energy*, **37**, 357 (2000).

[2] S. Shiroya, H. Unesaki and T. Misawa, "Accelerator-Driven Subcritical Reactors in Japanese Universities: Experimental Study Using the Kyoto University Critical Assembly," *Trans. Am. Nucl. Soc.*, Annu. Mtg., Milwaukee, Wisconsin, Jun. 17-21, p78-79, (2000). American Nuclear Society.

[3] S. Shiroya, *et al*., "Experimental Study on Accelerator Driven Subcritical Reactor using the Kyoto University Critical Assembly (KUCA)," *Proc. Int. Conf. on New Frontiers of Nucl. Technol.: Reactor Physics, Safety and High-Performance Computing* (PHYSOR2002), Seoul, Korea, Oct. 7-10, 7C-01, (2002). American Nuclear Society.

[4] S. Shiroya, A. Yamamoto, K. Shin, T. Ikeda, S. Nakano and H. Unesaki, "Basic Study on Accelerator Driven Subcritical Reactor in Kyoto University Research Reactor Institute (KURRI)," *Prog. Nucl. Energy*, **40**, 489 (2002).

[5] C. H. Pyeon, Y. Hirano, T. Misawa, H. Unesaki and S. Shiroya, "Preliminary Study on ADSR by using FFAG Accelerator in KUCA," *Proc. Embedded Topl. Mtg. Global2003*, New Orleans, Louisiana, Nov. 16-20, on CD-ROM, p 2193-2200, (2003). American Nuclear Society.

[6] H. Tagei, T. Iwasaki, T. Misawa and C. H. Pyeon, "Activation Experiment at KUCA for Establishing an Experimental Facility of Accelerator Driven Subcritical Reactor," *Proc. Int. Conf. on Nucl. Data for Sci. & Technol. – ND2004*, Santa Fe, New Mexico, Sep. 26-Oct. 1, on CD-ROM, (2004). American Nuclear Society.

[7] C. H. Pyeon, T. Misawa, H. Unesaki, S. Shiroya, H. Tagei, K. Wada and T. Iwasaki, "Experimental Analyses for Accelerator Driven Subcritical Reactor in Kyoto University Critical Assembly by using Foil Activation Method," *Proc. Int. Topl. Mtg. on Mathematics and Computation, Supercomputing, Reactor Physics and Nucl. Biological Applications* (M&C2005), Avignon, France, Sep. 12-15, on CD-ROM, (2005). American Nuclear Society.

[8] M. Hervault, C. H. Pyeon, T. Misawa, H. Unesaki and S. Shiroya, "Monte Carlo Analysis of Subcriticality for Accelerator Driven Subcritical Reactor Mock Up in Kyoto University Critical Assembly," *Proc. Int. Topl. Mtg. on Mathematics and Computation, Supercomputing, Reactor Physics and Nucl. Biological Applications* (M&C2005), Avignon, France, Sep. 12-15, on CD-ROM, (2005). American Nuclear Society.

[9] C. H. Pyeon, T. Misawa, H. Unesaki and S. Shiroya, "Present Status of Accelerator Driven Subcritical Reactor in Kyoto University Critical Assembly," *Proc. Int. Topl. Mtg. on Advanced in Nucl. Analysis and Simulation* (PHYSOR2006), Vancouver, Canada, Sep. 10-14, on CD-ROM, (2006). American Nuclear Society.

[10] H. Shiga, M. Hervault, C. H. Pyeon, T. Misawa and S. Shiroya, "Neutron Spectrum Analyses by using Foil Activation Method at Accelerator Driven Subcritical Reactor in Kyoto University Critical Assembly," *Proc. 2nd COE-INES Int. Sympo.* (INES-2), Yokohama, Japan, Nov. 28-30, on CD-ROM, (2006).

[11] M. Hervault, T. Kitada, H. Unesaki, C. H. Pyeon, T. Misawa and S. Shiroya, "Experiments for Accelerator Driven Subcritical Reactor with Optical Fiber Detectors and Pulsed Neutron Generator in Kyoto University Critical Assembly," *Proc. 1st Int. Conf. Physics & Technol. of Reactors & Applications* (PHYTRA-1), Caracas, Morocco, Mar. 14-16, on CD-ROM, (2007).

[12] C. H. Pyeon, T. Misawa, H. Unesaki and S. Shiroya, "Benchmark Experiments of Accelerator Driven Systems (ADS) in Kyoto University Critical Assembly (KUCA)," *Proc. Fifth Int. Workshop on the Utilisation and Reliability of High Power Proton Accelerators* (HPPA5), May, 6-9, Mol, Belgium, on CD-ROM, (2007). OECD/NEA.

[13] C. H. Pyeon, T. Misawa, H. Unesaki, C. Ichihara and K. Mishima, "Research on Accelerator Driven Subcritical Reactor at Kyoto University Critical Assembly (KUCA)," *Proc. Eighth Int. Topl. Mtg. on Nucl. Applications and Utilization of Accelerators* (AccApp'07), Jul. 30 - Aug. 2, Pocatello, on CD-ROM, (2007). American Nuclear Society.

[14] C. H. Pyeon, Y. Hirano, T. Misawa, H. Unesaki, C. Ichihara, T. Iwasaki and S. Shiroya, "Preliminary Experiments on Accelerator Driven Subcritical Reactor with Pulsed Neutron Generator in Kyoto University Critical Assembly," *J. Nucl. Sci. Technol.,* **44**, 1368 (2007).

[15] C. H. Pyeon, M. Hervault, T. Misawa, H. Unesaki, T. Iwasaki and S. Shiroya, "Static and Kinetic Experiments on Accelerator Driven Subcritical Reactor with 14 MeV Neutrons in Kyoto University Critical Assembly," *J. Nucl. Sci. Technol.,* **45**, 1171 (2008).

Experimental Benchmarks for Accelerator-Driven System (ADS) at Kyoto University Critical Assembly (KUCA) Phase I

Please submit results to:

Cheolho Pyeon
Research Reactor Institute, Kyoto University
2-1010, Asashiro-nishi, Kumatori-cho, Sennan-gun, Osaka 590-0494, Japan
Phone: +81-72-451-2356
Fax: +81-72-451-2603
E-mail: pyeon@rri.kyoto-u.ac.jp

Name:____

Affiliation:______________________________________

____

Address:_______________________________________

____

Phone:____

Fax: _______________________________________

E-mail:____

Please submit the results on the following forms or in a similar format. Include additional pages if necessary. Submission of partial results is acceptable, as is the submission of revised results.

Appendix

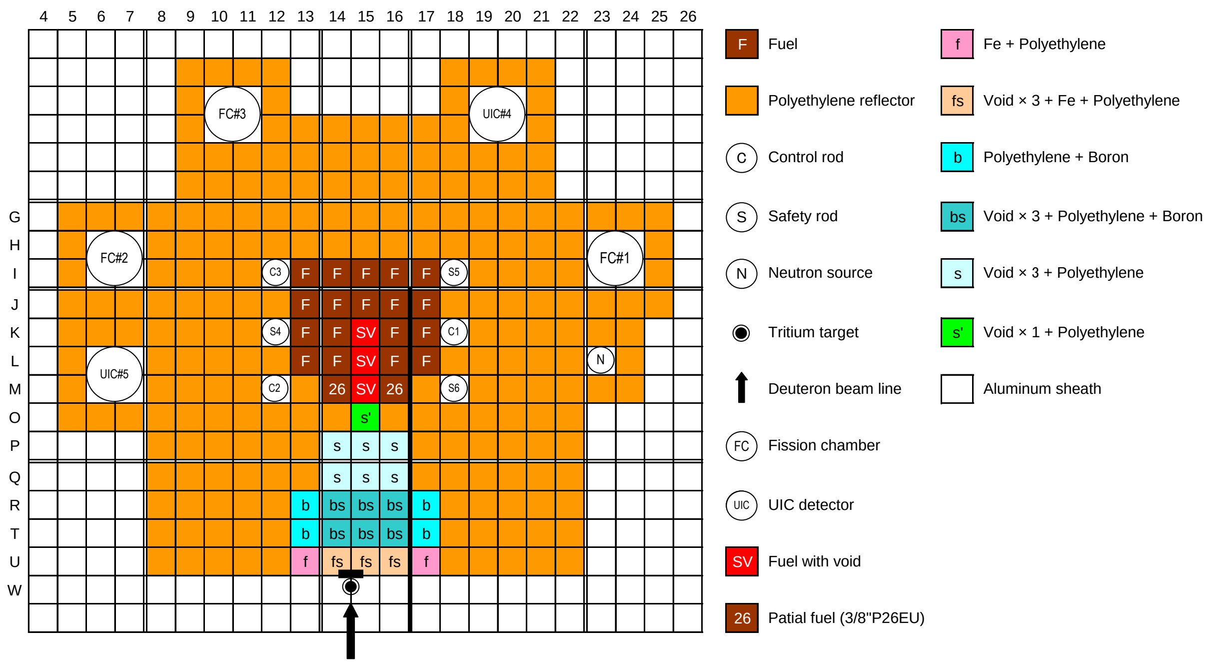

Fig. 1-1 The general view of KUCA core configuration.

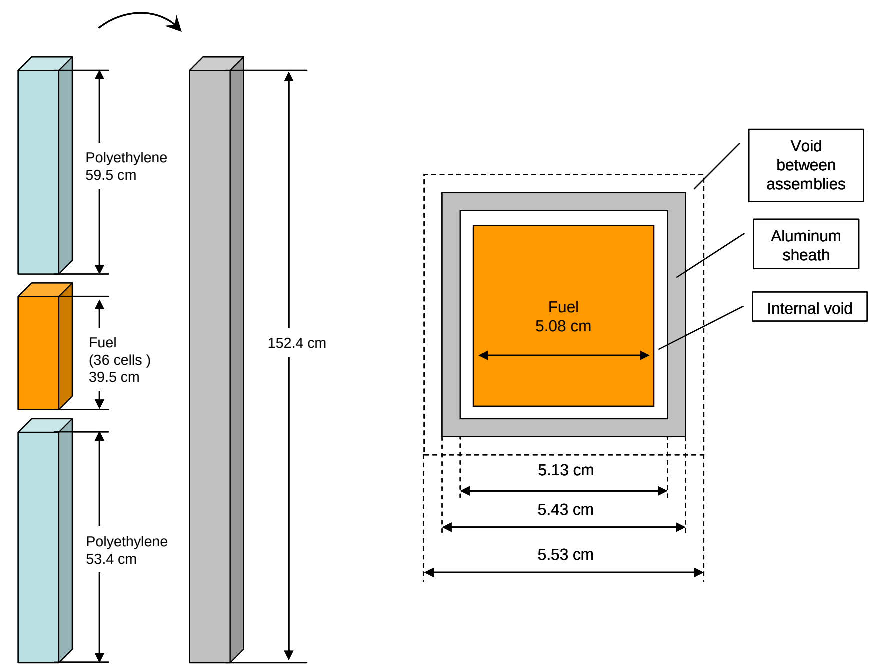

Fig. 1-2 Description of fuel assembly at KUCA.

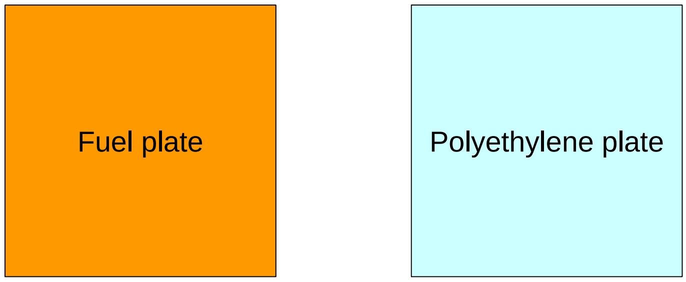

Fig. 1-3 Description of fuel and polyethylene plates.

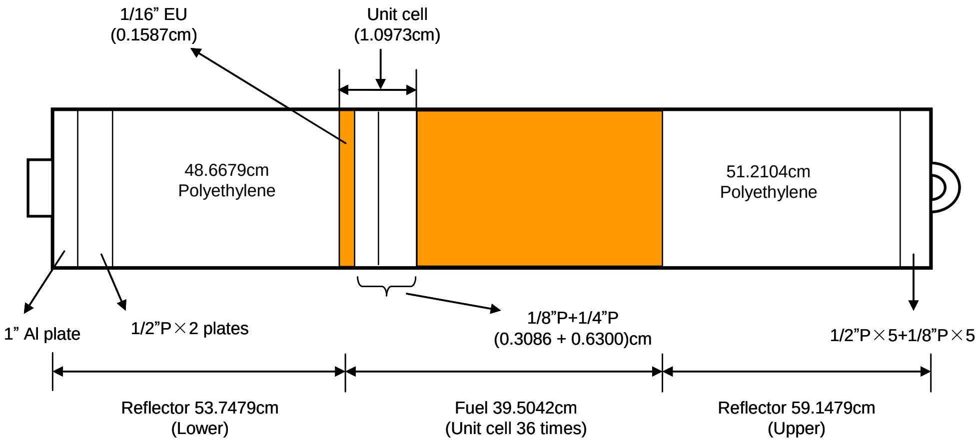

Fig. 1-4 Fall sideways view of fuel assembly "F" shown in Fig. 1-1.

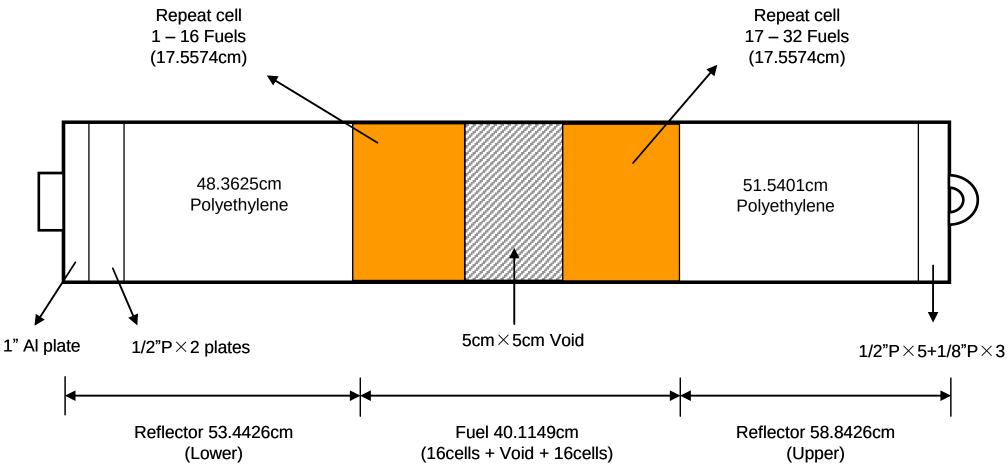

Fig. 1-5 Fall sideways view of fuel assembly "SV" with void shown in Fig. 1-1.

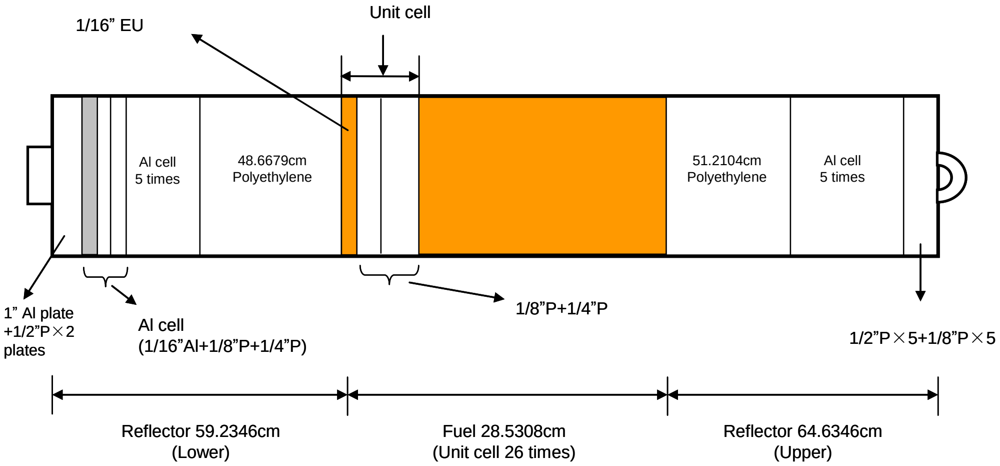

Fig. 1-6 Fall sideways view of partial fuel assembly "26" shown in Fig. 1-1

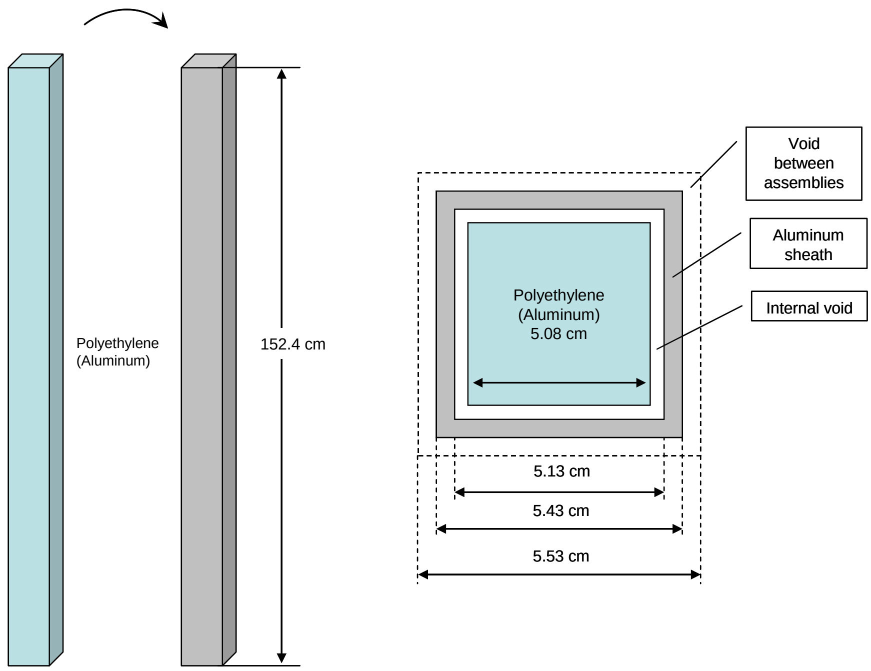

Fig. 1-7 Description of polyethylene (Aluminum) reflector at KUCA.

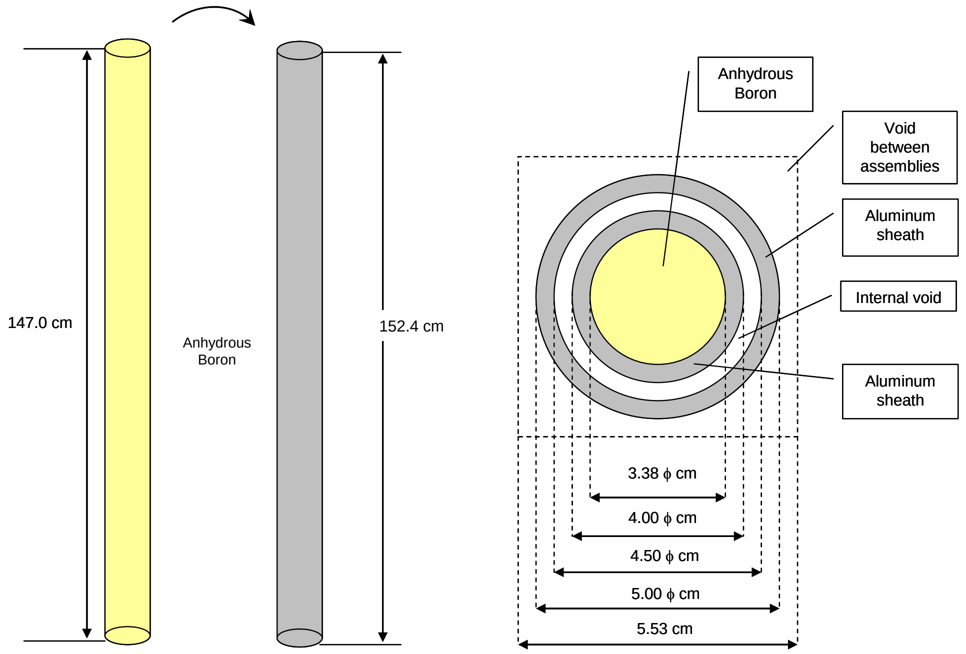

Fig. 1-8 Description of control (safety) rod at KUCA.

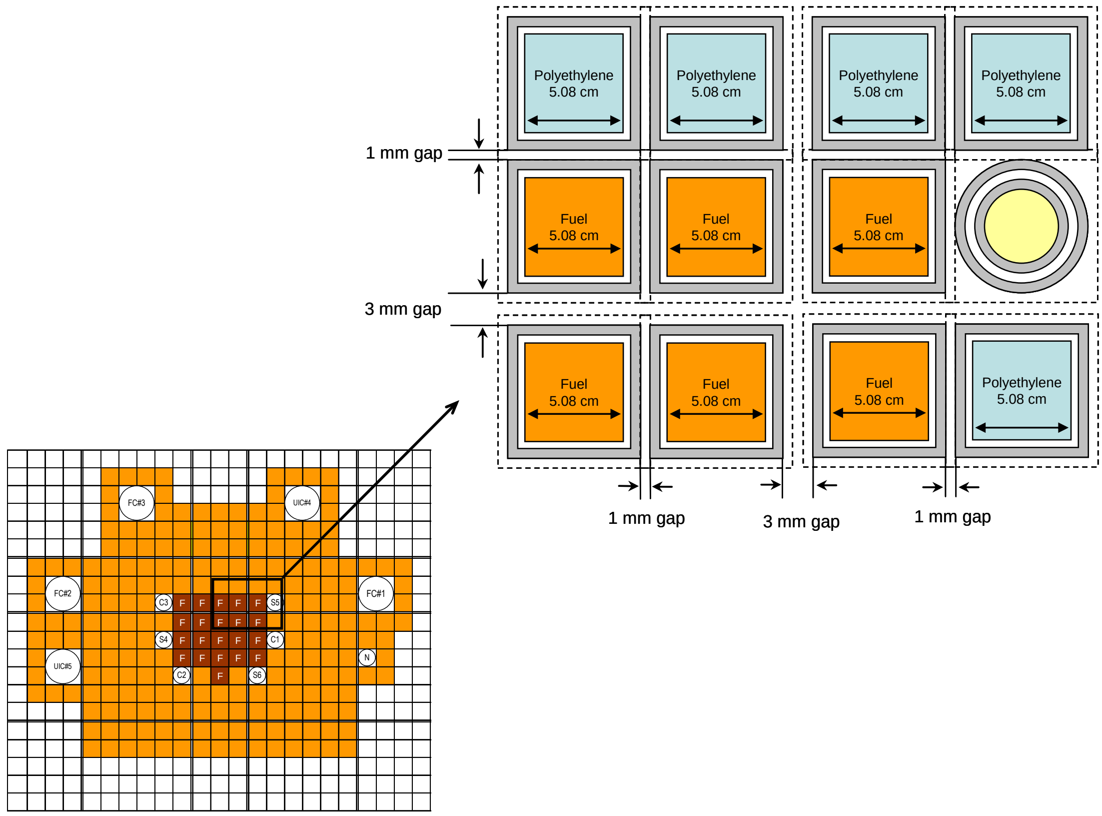

Fig. 1-9 Description of fuel assembly, polyethylene reflector and control rod at KUCA.

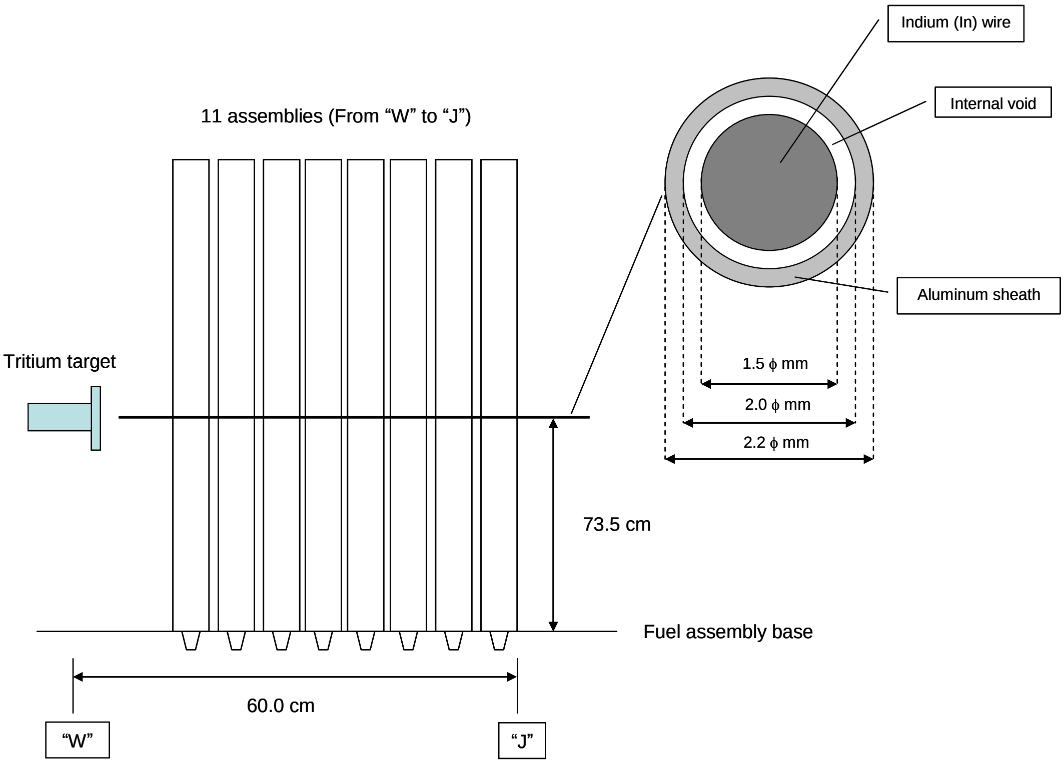

Fig. 1-10 Setting of Indium (In) wire.

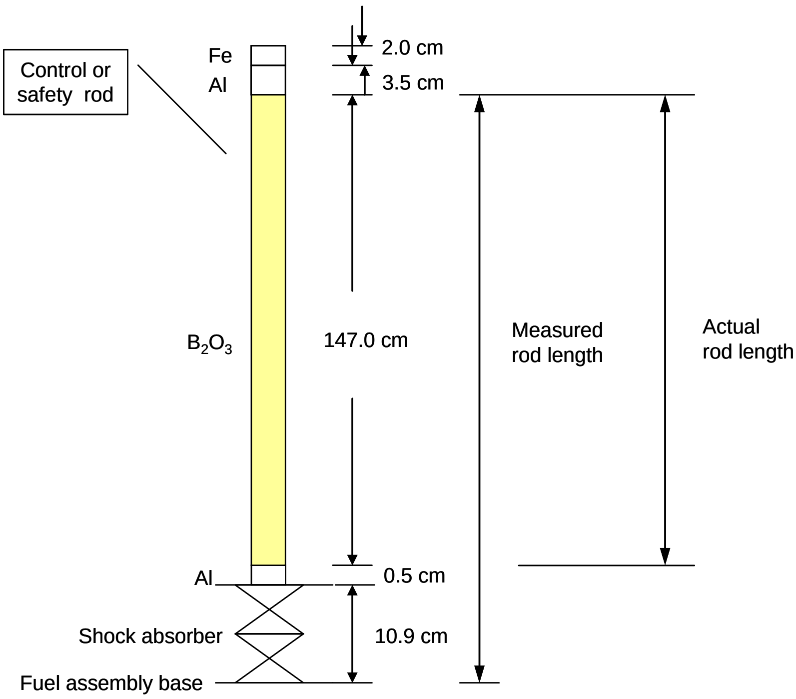

Fig. 1-11 Actual position of control (safety) rod.
(Actual position = Measured position – 11.4 cm)

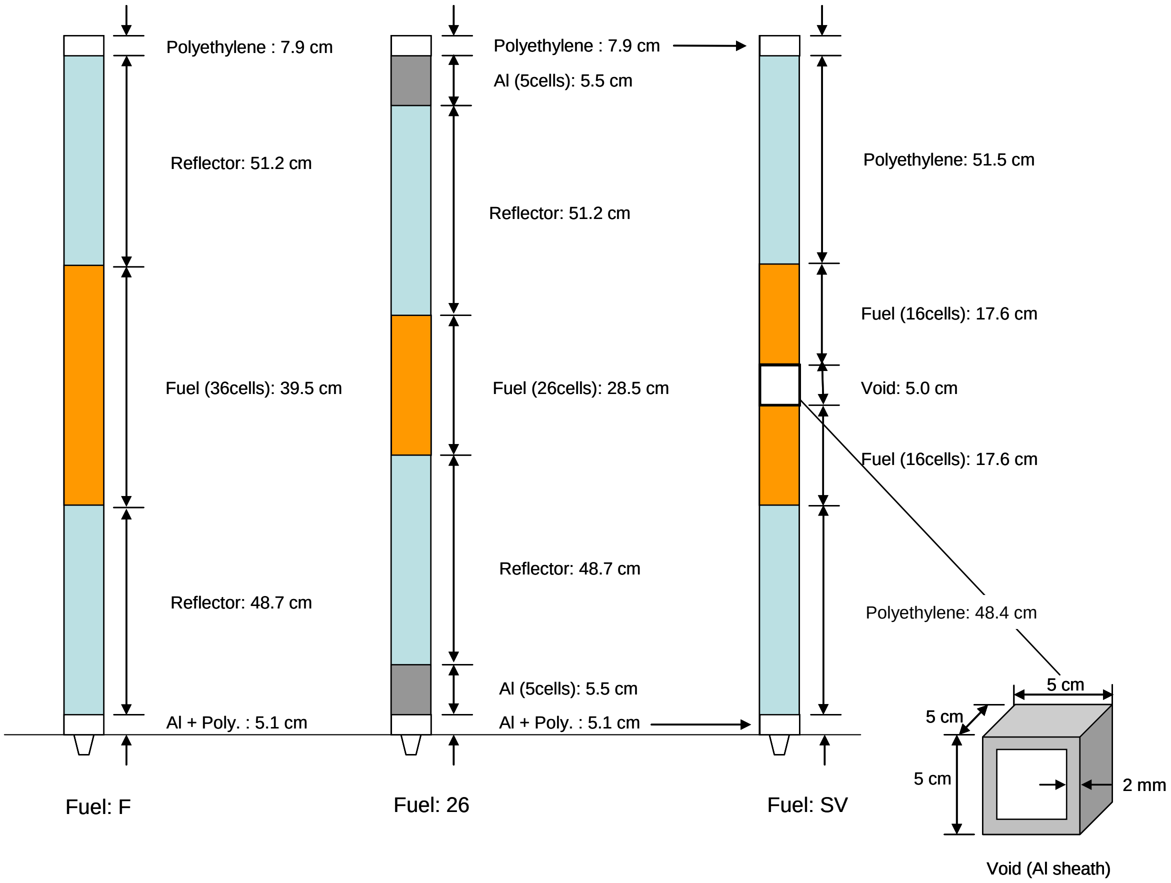

Fig. 1-12 Description of fuel “F,” partial fuel “26” and fuel “SV” assemblies shown in Fig. 1-1.

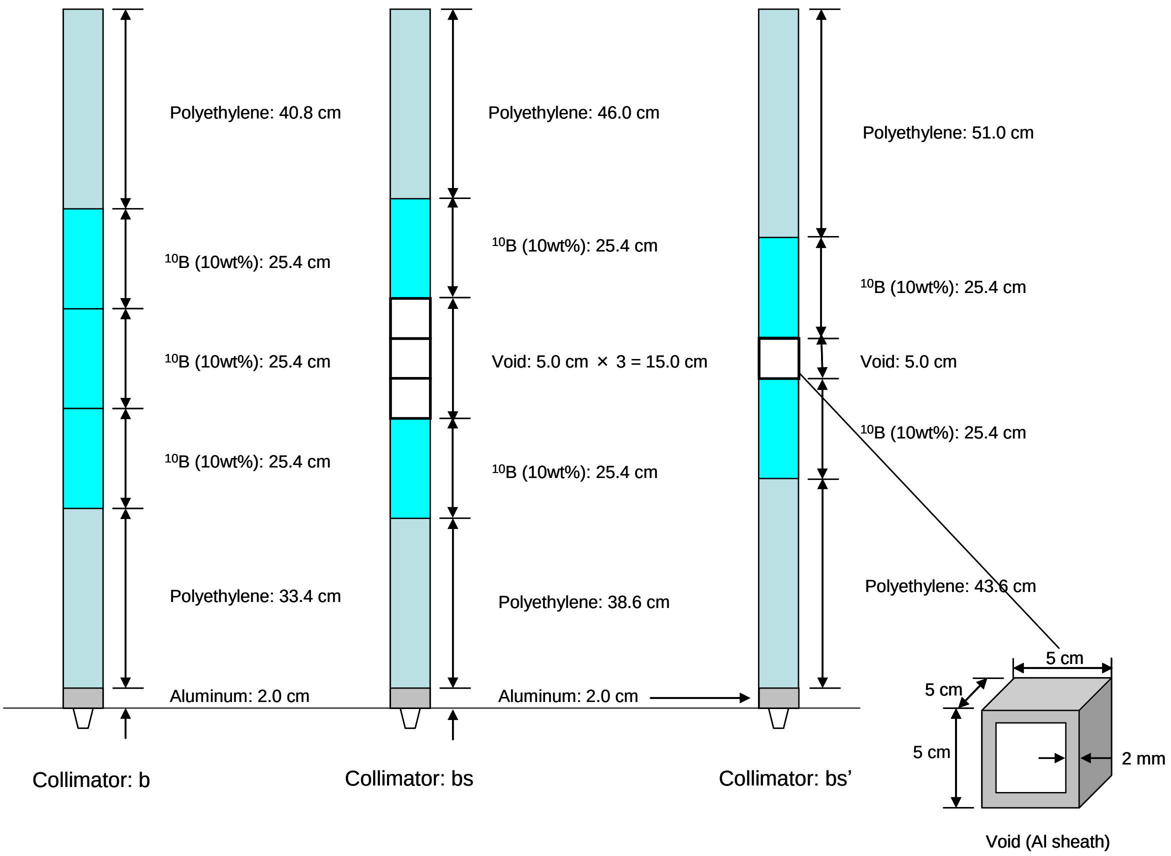

Fig. 1-13 Description of neutron shield and beam duct "b," "bs" and "bs'" shown in Fig. 1-1.

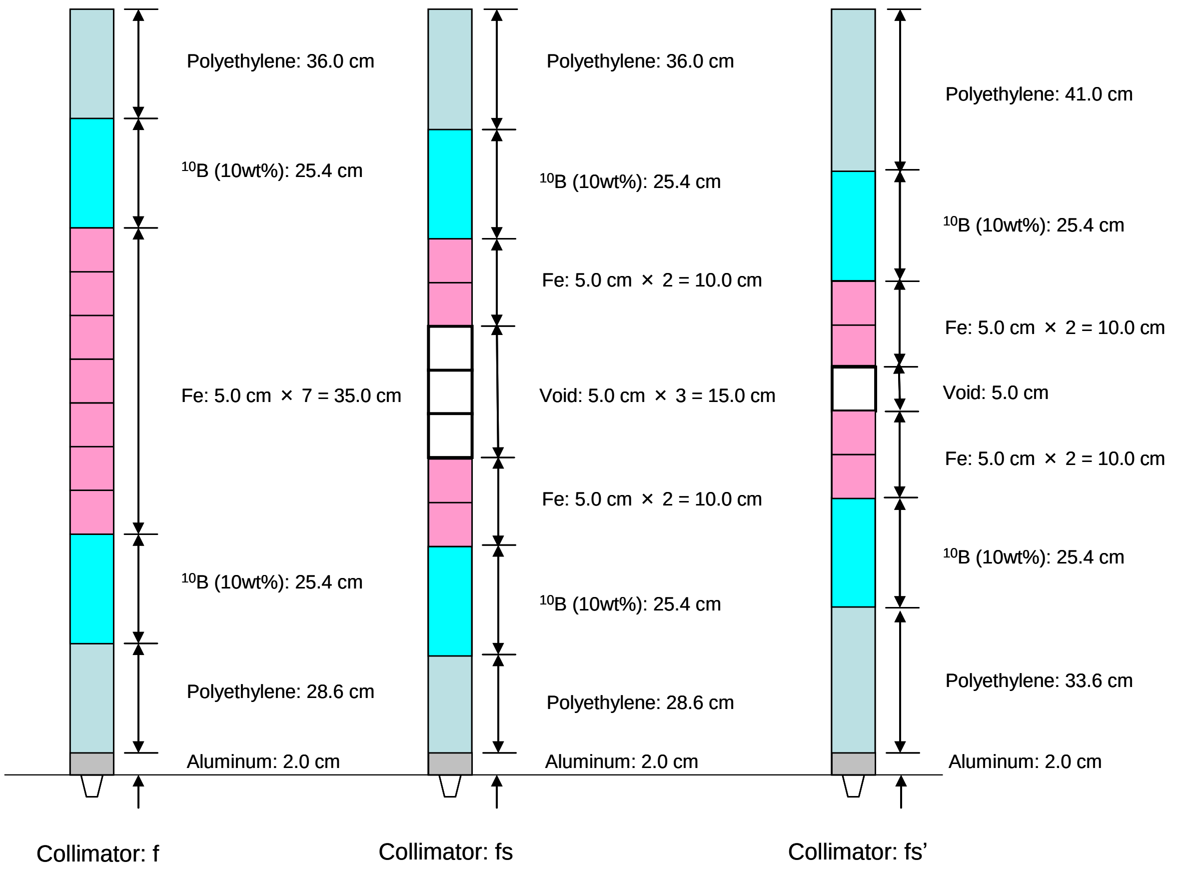

Fig. 1-14 Description of neutron shield and beam duct "f," "fs" and "fs'" shown in Fig. 1-1.

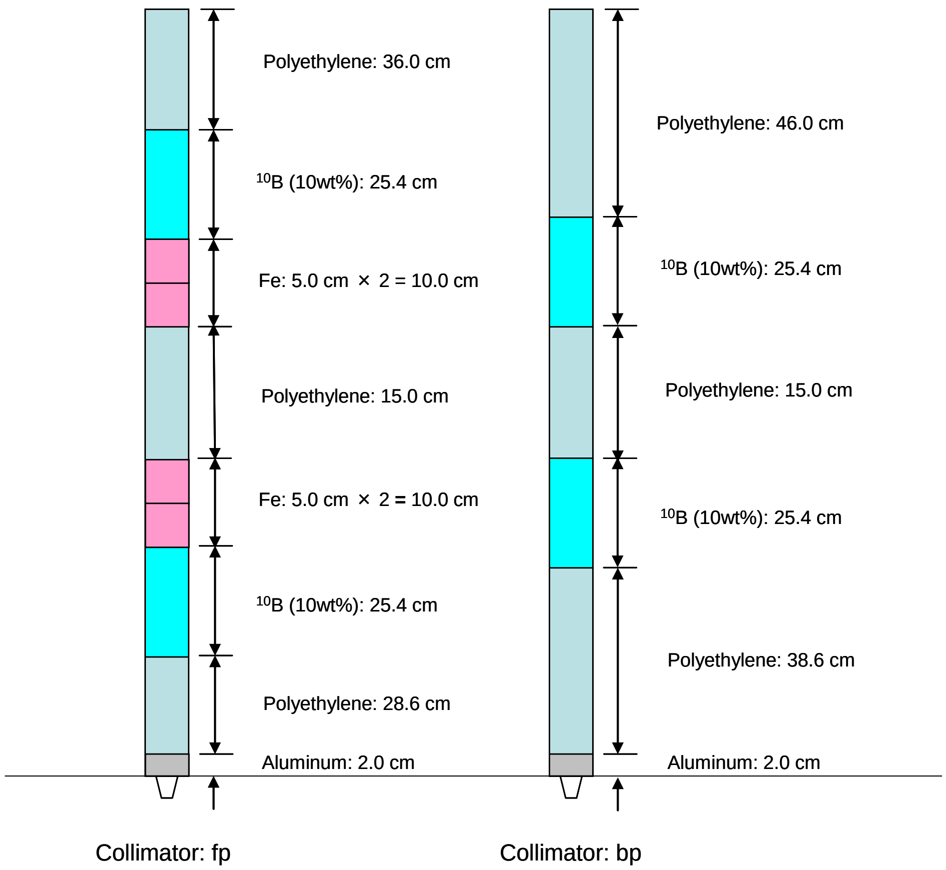

Fig. 1-15　Description of neutron shield "fp" and "bp."

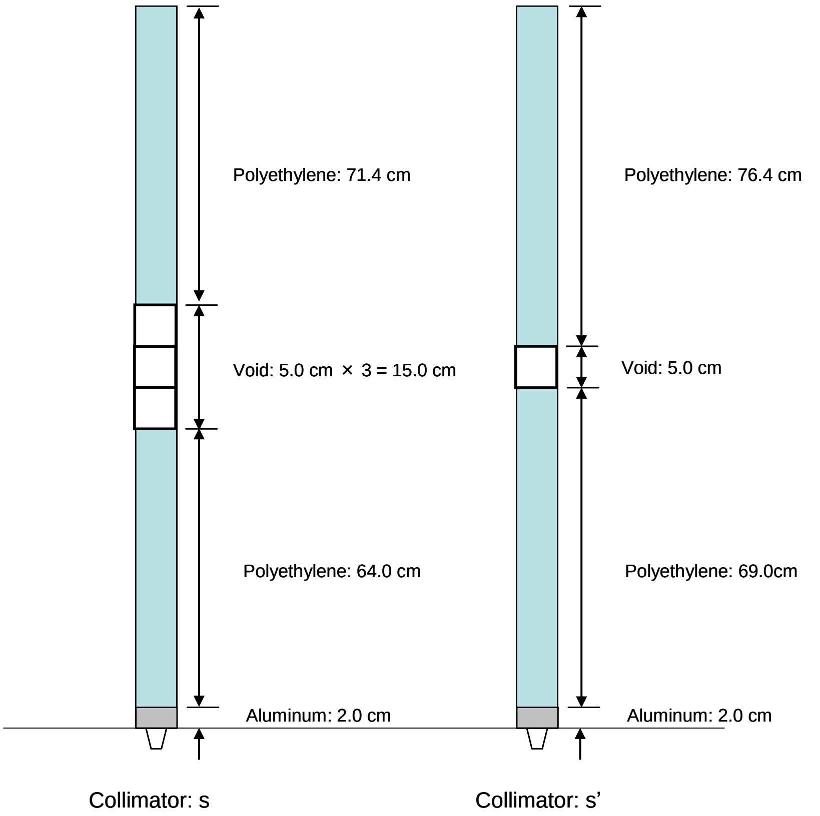

Fig. 1-16 Description of beam duct "s" and "s'" shown in Fig. 1-1.

Table I-1 Atomic densities of 1/16″ t highly enriched Uranium fuel plate made of U-Al alloy.

Isotope	Atomic density ($\times 10^{24}/cm^3$)
^{235}U	1.50694×10^{-3}
^{238}U	1.08560×10^{-4}
^{27}Al	5.56436×10^{-2}

Table I-2 Atomic densities of polyethylene reflector.

Isotope	Atomic density ($\times 10^{24}/cm^3$)			
	1/2″ t plate	1/4″ t plate	1/8″ t plate	Polyethylene square rod
^{1}H	8.06560×10^{-2}	8.08711×10^{-2}	8.02167×10^{-2}	8.00083×10^{-2}
^{6}C	4.03280×10^{-2}	4.04356×10^{-2}	4.01084×10^{-2}	4.00042×10^{-2}

Table I-3 Atomic densities of control and safety rods.

Isotope	Atomic density ($\times 10^{24}/cm^3$)
^{10}B	3.87448×10^{-3}
^{11}B	1.68447×10^{-2}
^{16}O	3.10787×10^{-2}

Table I-4 Atomic density of Aluminum sheath for the core element and 1/16″ t Al plate.

Isotope	Atomic density ($\times 10^{24}/cm^3$)
^{27}Al	6.00385×10^{-2}

Table I-5 Atomic densities of ^{10}B (10wt%) ^{56}Fe and ^{115}In shown in Fig. 13, 14 and 15.

Isotope	Atomic density ($\times 10^{24}/cm^3$)
^{1}H	7.02275×10^{-2}
^{12}C	3.60038×10^{-2}
^{10}B	8.97693×10^{-4}
^{11}B	3.90281×10^{-3}
^{16}O	7.20074×10^{-3}

Foil	Isotope	Abundance (%)	Purity (%)	Atomic density ($\times 10^{24}/cm^3$)
^{115}In	^{113}In	4.29	99.99	1.64406×10^{-3}
	^{115}In	95.71	99.99	3.66790×10^{-2}
^{56}Fe	^{54}Fe	5.845	99.5	4.93395×10^{-3}
	^{56}Fe	91.754	99.5	7.74524×10^{-2}
	^{57}Fe	2.119	99.5	1.78871×10^{-3}
	^{58}Fe	0.282	99.5	2.38045×10^{-4}

2. Core Configuration

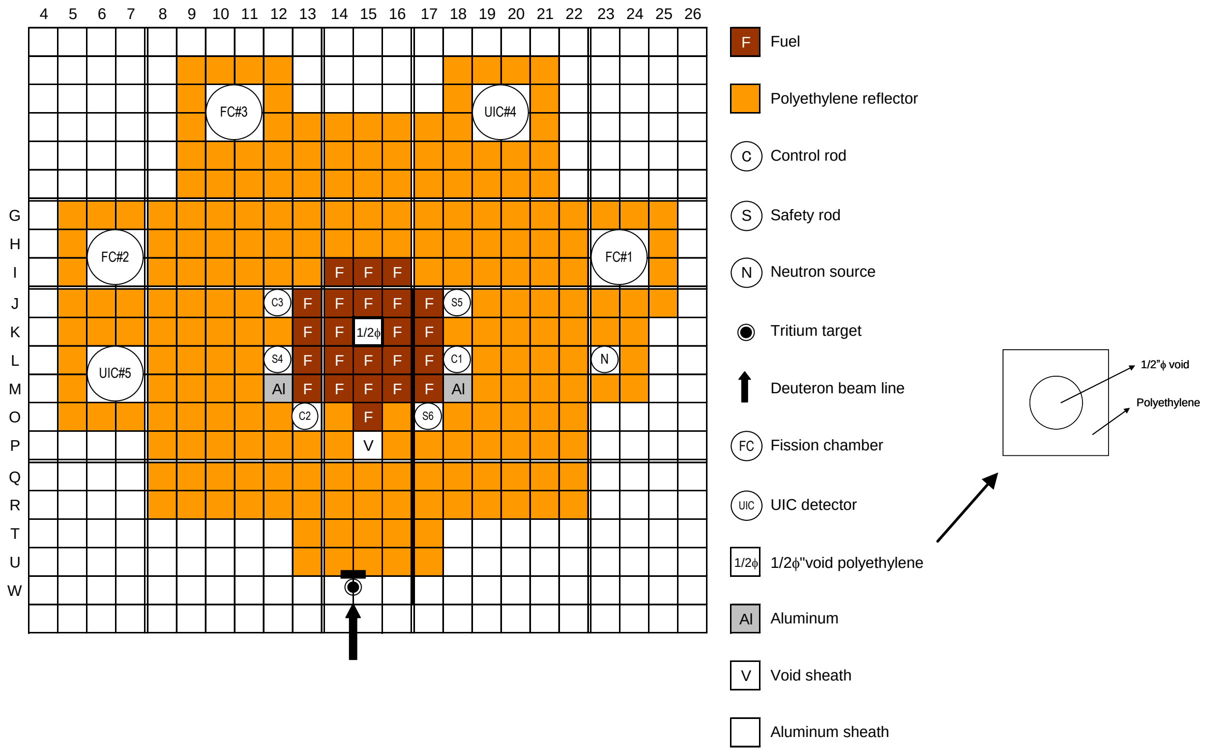

Fig. 2-1 No neutron shield and no beam duct core (Series-I: Case I-1).

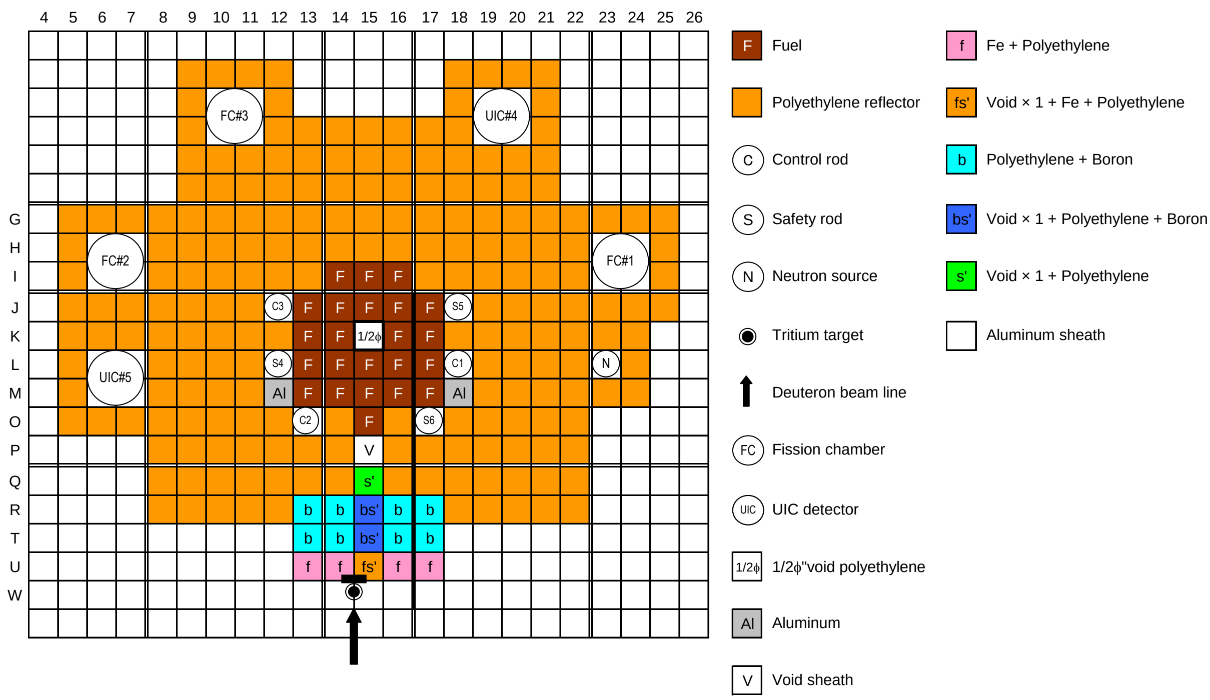

Fig. 2-2 Neutron shield and small beam duct (s') core (Series-I: Case I-2).

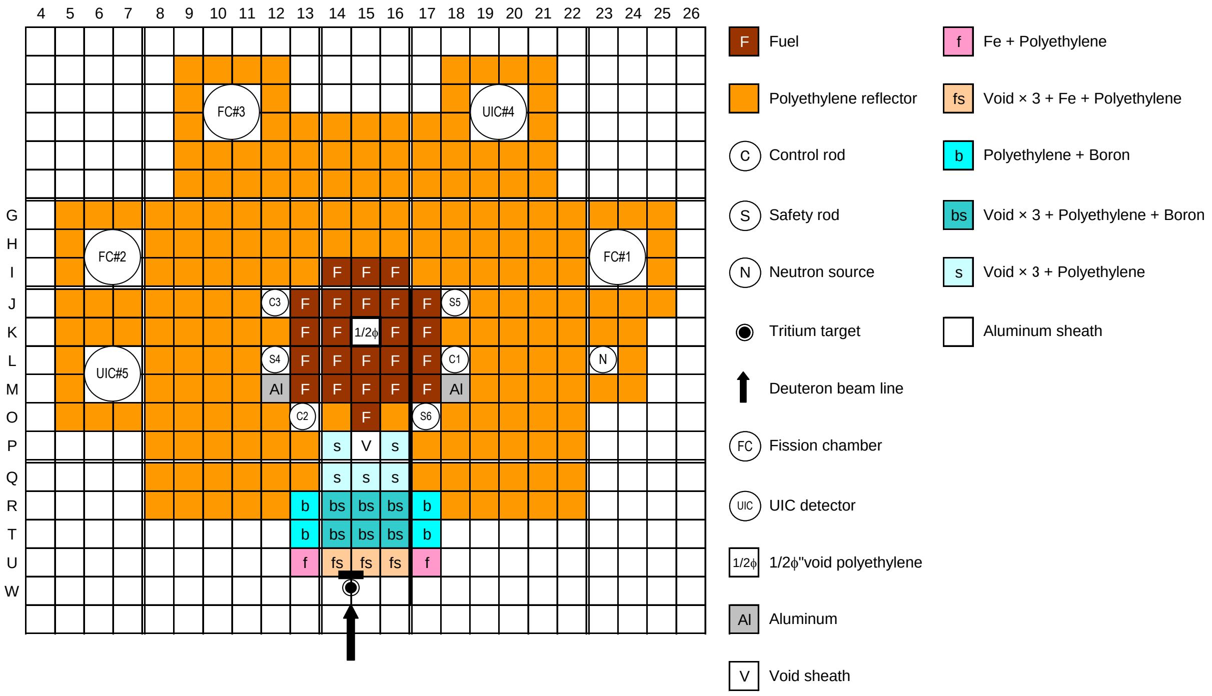

Fig. 2-3 Neutron shield and large beam duct (s) core (Series-I: Case I-3).

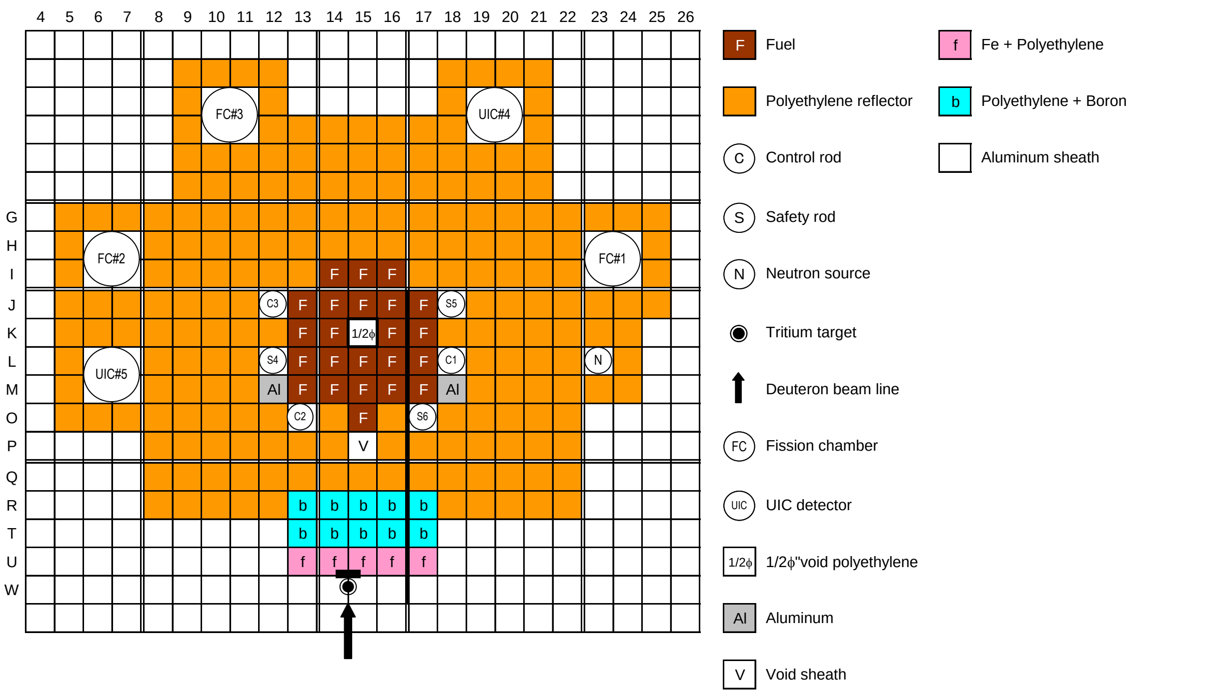

Fig. 2-4 Neutron shield and no beam duct core (Series-I: Case I-4).

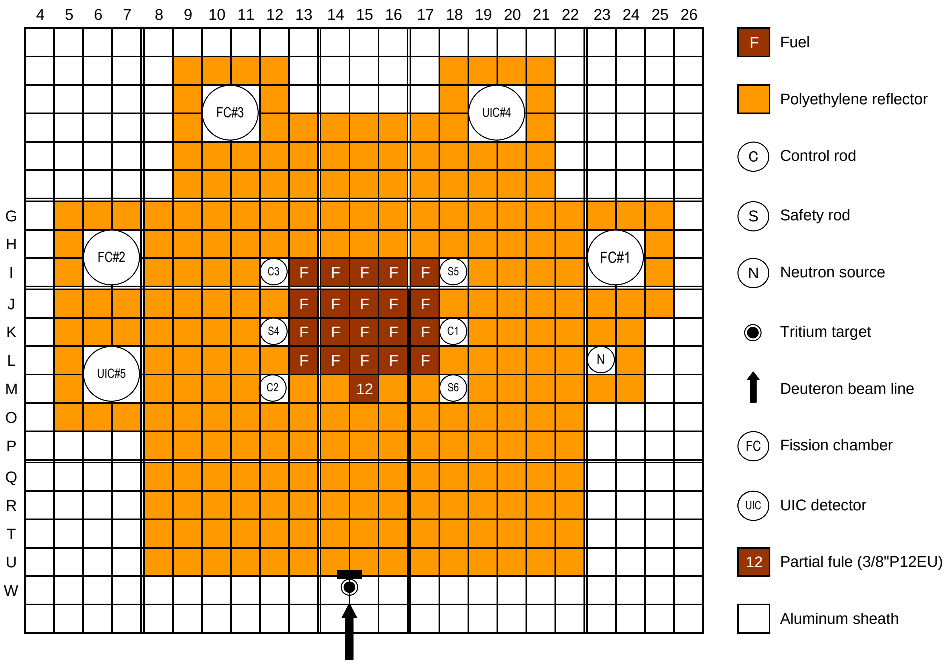

Fig. 2-5 No neutron shield, no beam duct and no SV core (Series-II: Case II-1).

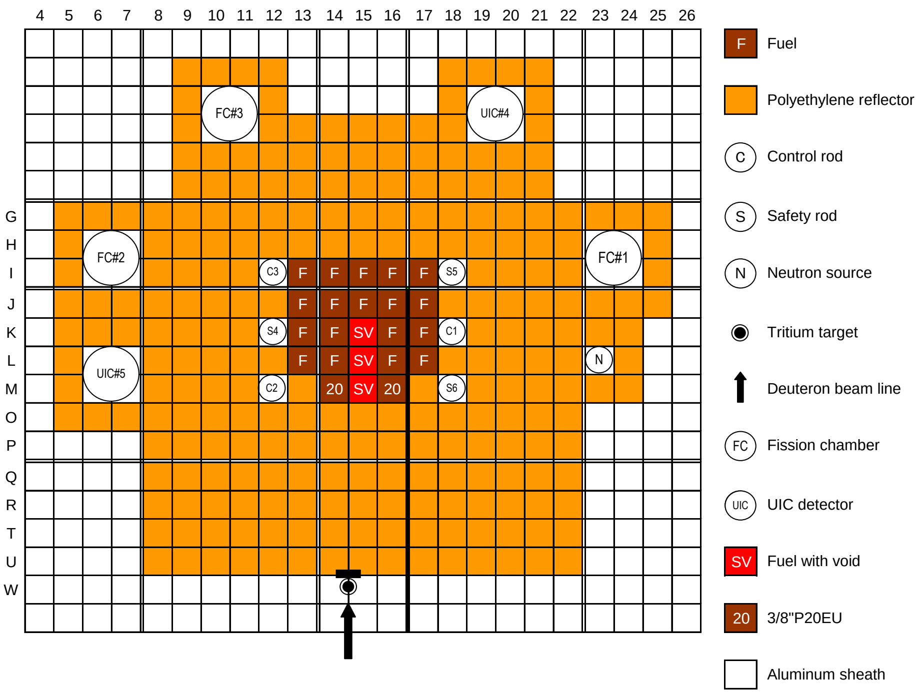

Fig. 2-6 No neutron shield, no beam duct and SV core (Series-II: Case II-2).

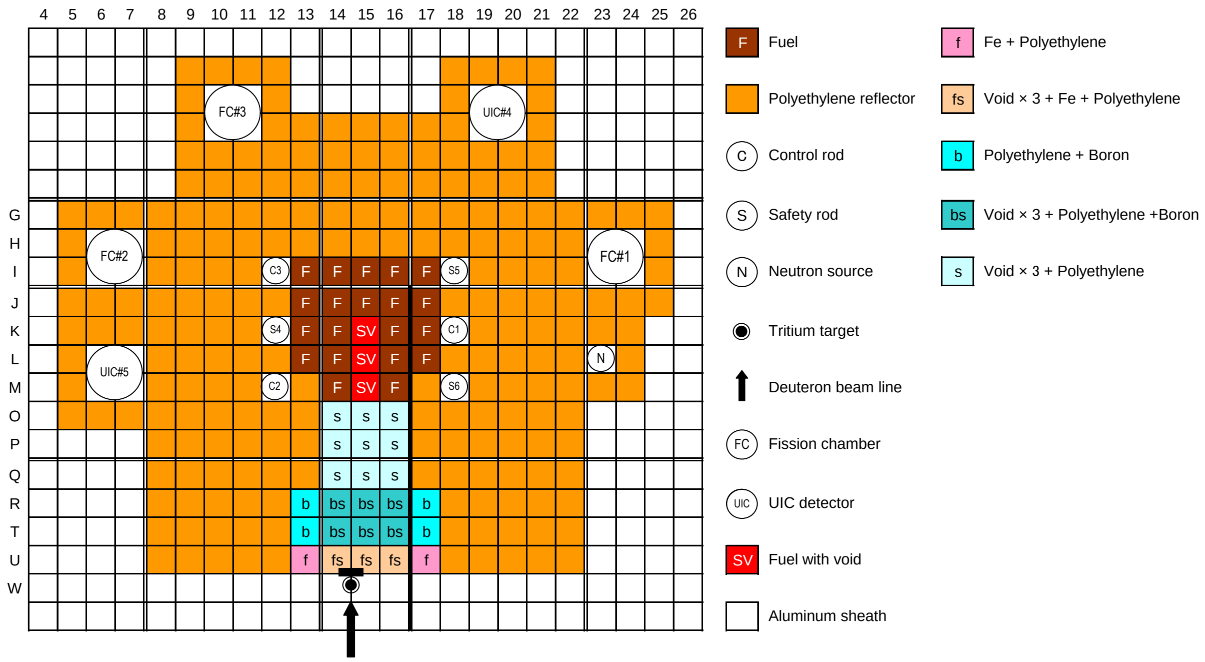

Fig. 2-7 Neutron shield, large beam duct (s) and SV core (Series-II: Case II-3).

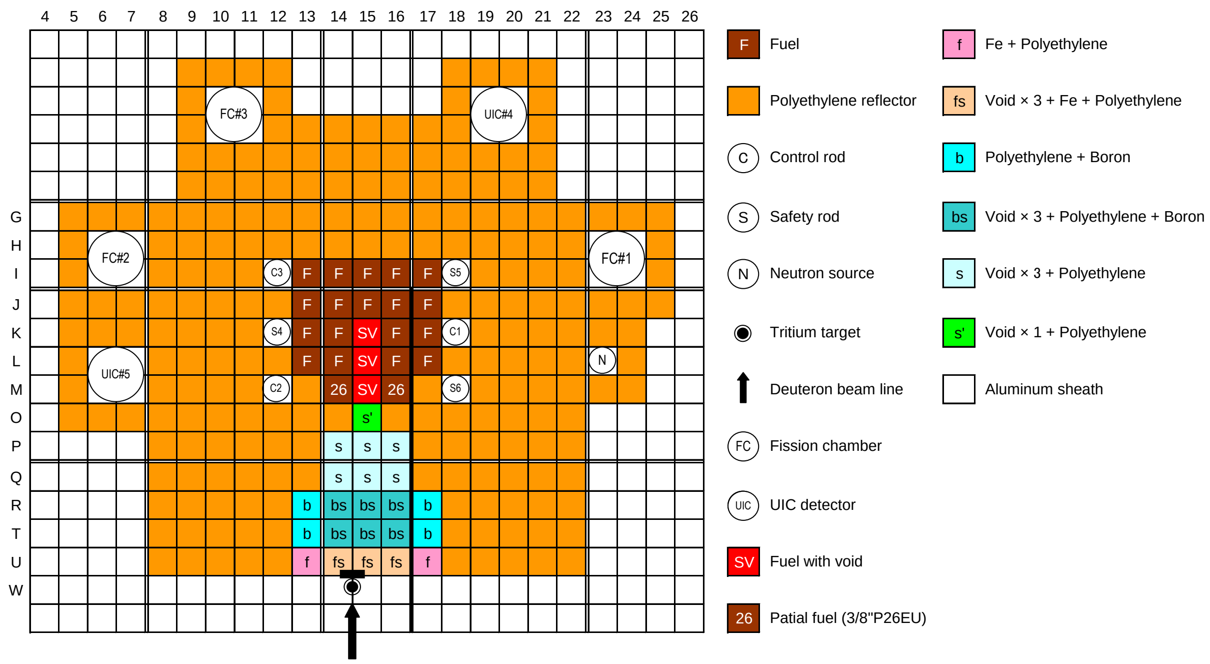

Fig. 2-8 Neutron shield, small beam duct (s’) and SV core (Series-II: Case II-4).

3. Results of ADS Experiments

3-1. Excess reactivity and Subcriticality

Table III-1 Measured excess reactivity and subcriticality obtained by control rod calibration curve, and control rod worth and its calibration curve, respectively.

Case name	Insertion rods pattern	Excess (%Δk/k)	Subcriticality (%Δk/k)
I-1	C1, C2, C3	0.295±0.021	0.904±0.063
I-2	C1, C2, C3	0.293±0.021	0.925±0.065
I-3	C1, C2, C3	0.020±0.001	1.171±0.082
I-4	C1, C2, C3	0.296±0.021	0.907±0.063
II-1	C1, C2, C3	0.143±0.010	0.793±0.056
II-2	C1, C2, C3	0.246±0.017	0.677±0.047
II-3	C1, C2, C3	0.037±0.003	0.893±0.063
II-4	C1, C2, C3	0.232±0.016	0.702±0.049
III-1	C1, C2, C3	0.050±0.004	0.850±0.060
III-2	C1, C2, C3, S4, S5, S6	0.049±0.003	1.751±0.123
III-3	C1, C2, C3, S5, S6	0.077±0.005	1.223±0.086

3-2. Reaction rate distribution

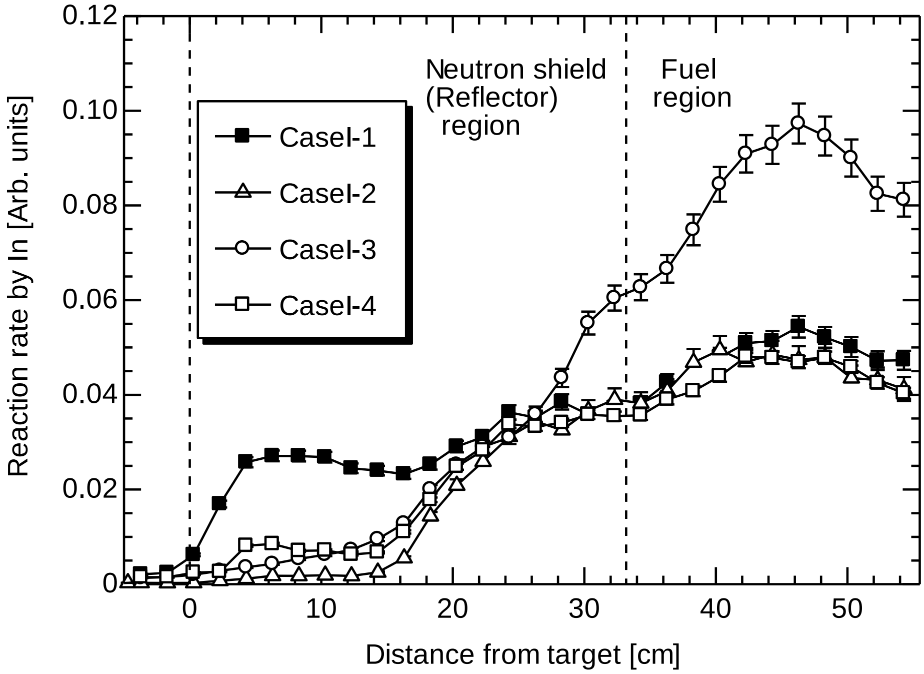

Fig. 3-1 Measured reaction rate distributions by Indium wire along vertical direction shown in Figs. 2-1 to 2-4 (Case I-1 to Case I-4).

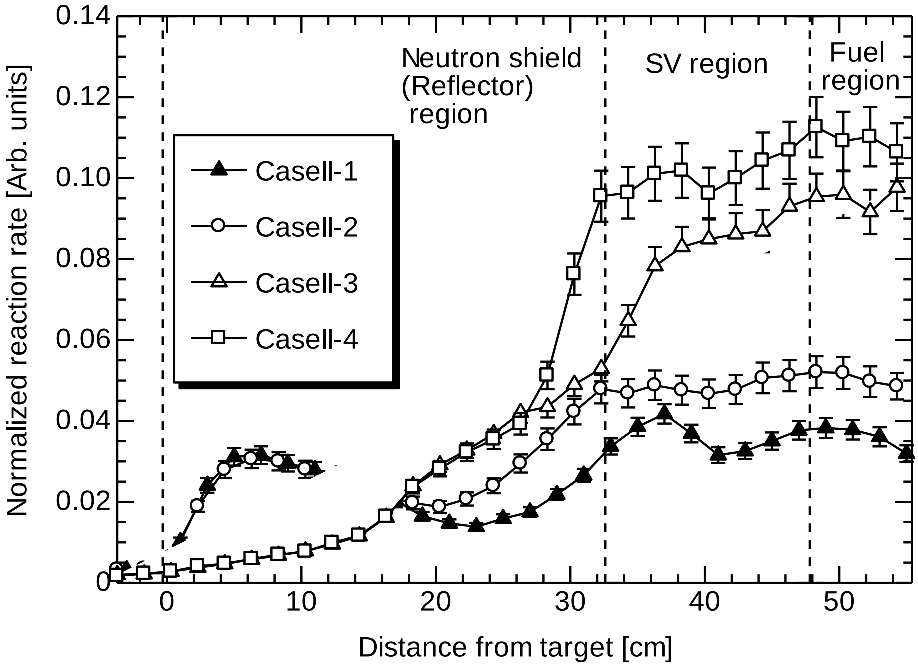

Fig. 3-2 Measured reaction rate distributions by Indium wire along vertical direction shown in Figs. 2-5 to 2-8 (Case II-1 to Case II-4).

3-3. Reaction rates of Activation foils

Table III-2 Measured reaction rates of activation foils on subcriticality 0.85%Δk/k (Case III-1) at position of (15, K) shown in Fig. 2-8.

Foil	Reaction	Saturation radioactivity (1/sec/cm^3)
^{115}In	(n, n')	$(3.160\pm0.036)\times10^3$
^{56}Fe	(n, p)	$(3.749\pm0.037)\times10^2$
^{27}Al	(n, α)	$(4.139\pm0.072)\times10^1$
^{93}Nb	(n, 2n)	—
^{197}Au	(n, γ)	$(3.516\pm0.034)\times10^5$

Table III-3 Measured reaction rates of activation foils on subcriticality 1.75%Δk/k (Case III-2) at position of (15, K) shown in Fig. 2-8.

Foil	Reaction	Saturation radioactivity (1/sec/cm^3)
^{115}In	(n, n')	$(1.238\pm0.015)\times10^3$
^{56}Fe	(n, p)	$(1.750\pm0.018)\times10^2$
^{27}Al	(n, α)	$(3.573\pm0.042)\times10^1$
^{93}Nb	(n, 2n)	—
^{197}Au	(n, γ)	$(1.582\pm0.014)\times10^5$

Table III-4 Measured reaction rates of activation foils on subcriticality 1.22%Δk/k (Case III-3) at the position of (15, K) shown in Fig. 2-8.

Foil	Reaction	Saturation radioactivity ($1/sec/cm^3$)
^{115}In	(n, n′)	$(2.085 \pm 0.023) \times 10^3$
^{56}Fe	(n, p)	$(3.139 \pm 0.030) \times 10^2$
^{27}Al	(n, α)	$(4.513 \pm 0.092) \times 10^1$
^{93}Nb	(n, 2n)	$(3.389 \pm 0.172) \times 10^2$
^{197}Au	(n, γ)	$(5.532 \pm 0.051) \times 10^5$

Table III-5 Measured reaction rates of activation foils at the position of target shown in Fig. 2-8.

Foil	Reaction	Saturation radioactivity ($1/sec/cm^3$)
^{115}In	(n, n′)	$(5.164 \pm 0.051) \times 10^3$
^{56}Fe	(n, p)	$(3.661 \pm 0.032) \times 10^3$
^{27}Al	(n, α)	$(6.125 \pm 0.044) \times 10^3$
^{93}Nb	(n, 2n)	$(2.487 \pm 0.028) \times 10^4$
^{93}Nb*	(n, 2n)	$(2.081 \pm 0.028) \times 10^4$

*: Normalization foil

Table III-6 Atomic density of activation foils utilized in reaction rates measurement.

Foil	Isotope	Abundance (%)	Purity (%)	Atomic density ($\times 10^{24}/cm^3$)
^{115}In	^{113}In	4.29	99.99	1.64406×10^{-3}
	^{115}In	95.71	99.99	3.66790×10^{-2}
^{56}Fe	^{54}Fe	5.845	99.5	4.93395×10^{-3}
	^{56}Fe	91.754	99.5	7.74524×10^{-2}
	^{57}Fe	2.119	99.5	1.78871×10^{-3}
	^{58}Fe	0.282	99.5	2.38045×10^{-4}
^{27}Al	^{27}Al	100	99.5	5.99156×10^{-2}
^{93}Nb	^{93}Nb	100	99.9	5.54750×10^{-2}
^{197}Au	^{197}Au	100	99.95	5.90193×10^{-2}

4. Core Condition

Table IV-1 Core condition of all the cases, including foils, neutrons shield, SV, In wire, partial fuel and control rods positions.

Case	Foils No.	Neutron shield	SV fuel	In wire	Partial fuel	C1 (mm)	C2 (mm)	C3 (mm)	S4-S6 (mm)
Case I-1	×	×	×	○	×	U.L.	U.L.	524.34	U.L.
Case I-2	×	○ (s)	×	○	×	U.L.	U.L.	548.21	U.L.
Case I-3	×	○ (s')	×	○	×	U.L.	U.L.	745.54	U.L.
Case I-4	×	○ (s_NV)*	×	○	×	U.L.	U.L.	525.52	U.L.
Case II-1	×	×	×	○	12	U.L.	U.L.	635.94	U.L.
Case II-2	1	×	○	○	20	637.48	U.L.	U.L.	U.L.
Case II-3	1	○ (s)	○	○	36	U.L.	U.L.	742.48	U.L.
Case II-4	1	○ (s')	○	○	26	U.L.	U.L.	553.24	U.L.
Case III-1	2	○ (s')	○	○	20	U.L.	U.L.	725.35	U.L.
Target	3								
Case III-2	2	○ (s')	○	○	20	U.L.	U.L.	727.36	U.L.
Target	3								
Case III-3	2	○ (s')	○	○	20	U.L.	U.L.	694.11	U.L.
Target	3								

*: No void (NV)

Foils No.: Refer to Table IV-2

U.L.: Upper Limit (1,200 mm)

Table IV-2 Foil Selection utilized in neutron spectrum experiments.

Case	Foils No.								
Case II	1	Ni	Al	Fe	In				
	Normalization foil (at target)					In*			
Case III	2		Al	Fe	In		Nb		Au
	Normalization foil (at target)							Nb*	
Target	3		Al	Fe	In		Nb	Nb*	

Table IV-3 Size of activation foil.

Foil	Size
Ni	45mm*45mm*5mm
Al	45mm*45mm*5mm
Fe	45mm*45mm*5mm
In	45mm*45mm*3mm
In*	20mm*20mm*1mm
Nb	45mm*45mm*2mm
Nb*	50mm*50mm*1mm
Au	20mm*20mm*1mm

Experimental Benchmarks for Accelerator-Driven System (ADS) at Kyoto University Critical Assembly (KUCA)

Phase 2 (Results)

Kyoto University Research Reactor Institute, Japan

Cheolho Pyeon

5. Neutron noise method (Feynmann-α and Rossi-α methods)

Table V-1 Control and safety rod positions on the subcriticality measurement

Case	C1	C2	C3	S4	S5	S6
I-1	0.0	0.0	1200.0	1200.0	1200.0	1200.0
I-2	0.0	0.0	1200.0	0.0	1200.0	1200.0
I-3	0.0	0.0	0.0	1200.0	0.0	0.0
I-4	0.0	0.0	0.0	0.0	0.0	0.0

Table V-2 Measured subcriticality (%Δk/k) using neutron noise method shown in Fig. 5-1 (pulsed period 20 (ms))

Case	Subcriticality (%Δk/k)	Reference* α (1/sec)	Feynman** α (1/sec)	Feynman*** α (1/sec)	Rossi (1/sec)
I-1	0.50±0.01	266±2	253±1	285±1	263±1
I-2	0.99±0.01	369±3	373±2	383±1	368±2
I-3	1.58±0.02	494±3	495±3	508±1	500±5
II-4	2.07±0.02	598±4	601±4	631±2	599±7

*: Reference α was obtained using pulsed neutron method.
**: Stochastic Feynman-α
***: Deterministic Feynman-α
Note that the calculated values of β_{eff} and l are 7.627×10^{-3} and 4.304×10^{-5} (sec), respectively, in this core.

Table V-3 Measured subcriticality (%Δk/k) using neutron noise method shown in Fig. 5-1 (pulsed period 10 (ms))

Case	Subcriticality (%Δk/k)	Reference* α (1/sec)	Feynman** α (1/sec)	Feynman*** α (1/sec)	Rossi (1/sec)
I-1	0.50±0.01	266±2	262±1	310±1	259±1
I-2	0.99±0.01	369±3	360±2	397±1	363±2
I-3	1.58±0.02	494±3	463±3	530±1	485±5
I-4	2.07±0.02	598±4	585±6	641±2	600±14

Table V-4 Measured subcriticality (%Δk/k) using neutron noise method shown in Fig. 5-1 (pulsed period 1 (ms))

Case	Subcriticality (%Δk/k)	Reference* α (1/sec)	Feynman** α (1/sec)	Feynman*** α (1/sec)	Rossi (1/sec)
I-1	0.50±0.01	266±2	258±1	None	260±1
I-2	0.99±0.01	369±3	367±1	None	370±2
I-3	1.58±0.02	494±3	507±2	None	502±3
I-4	2.07±0.02	598±4	604±3	None	601±6

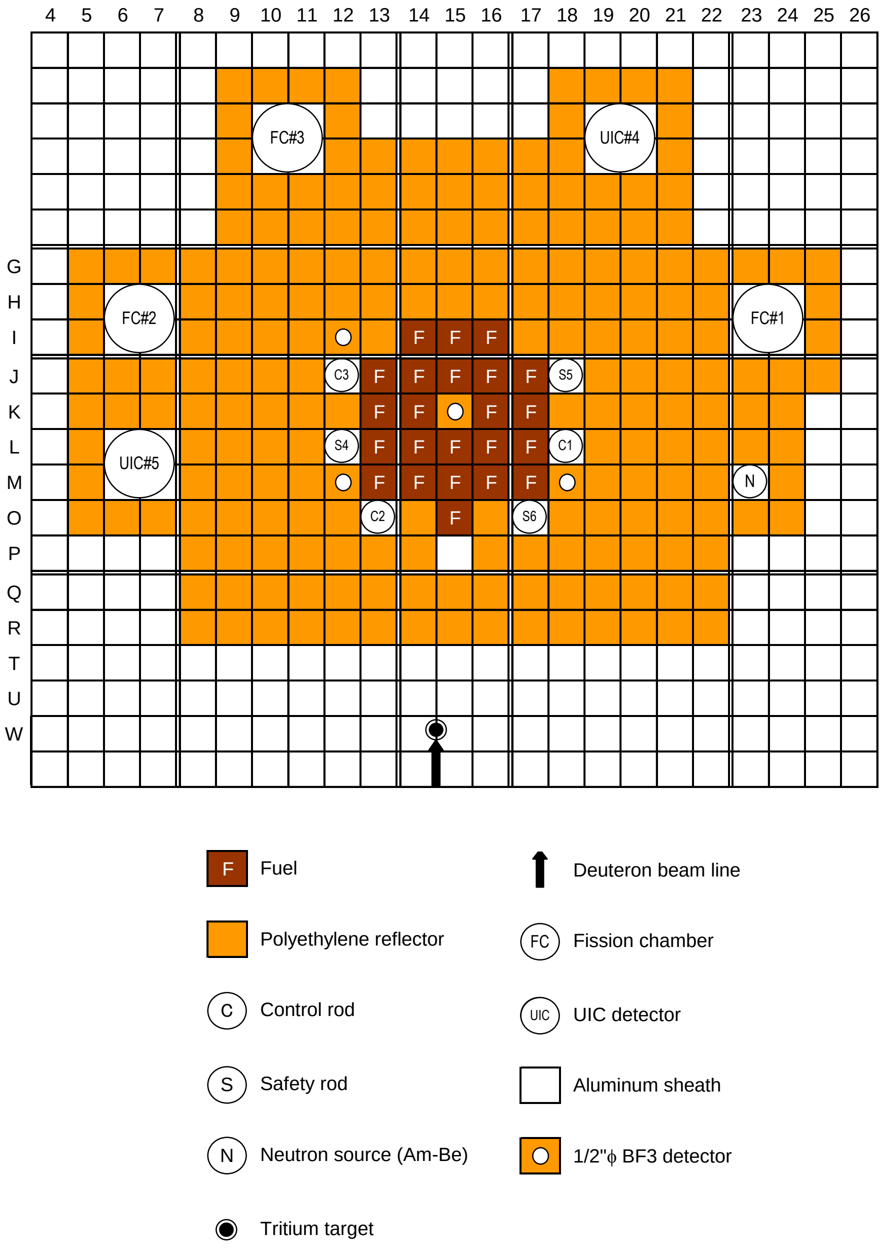

Fig. 5-1 Core configuration of subcriticality measurement using neutron noise method (Cases I-1 through I-4)

6. Source multiplication method

6-1 Cases II-1 through II-4

Table VI-1 Control and safety rod positions in subcriticality system and reference subcriticality by measurement

Case	Rod pattern	Subcriticality (%Δk/k)
II-1	C1, C2, C3, S4, S5, S6 (All rod positions: 650 mm)	1.00±0.01
II-2	C1, C2, C3, S4, S5, S6 (All rod positions: 580 mm)	1.50±0.02
II-3	C1, C2, C3, S4, S5, S6 (All rod positions: 510 mm)	2.00±0.02
II-4	C1, C2, C3, S4, S5, S6 (All rod positions: Lower limit)	2.28±0.02

Table VI-2 Measured subcriticality (%Δk/k) using source multiplication method at each detector position shown in Fig. 2-1

Case	(15, K)	(20, I)	(20, K)	(20, L)	(20, O)
II-1	0.89±0.01	0.95±0.01	0.99±0.01	0.96±0.01	0.94±0.01
II-2	1.54±0.02	1.77±0.02	1.99±0.02	1.89±0.02	1.79±0.02
II-3	2.06±0.02	2.47±0.02	2.84±0.03	2.74±0.02	2.56±0.02
II-4	2.38±0.02	2.91±0.02	3.39±0.03	3.26±0.02	3.03±0.03

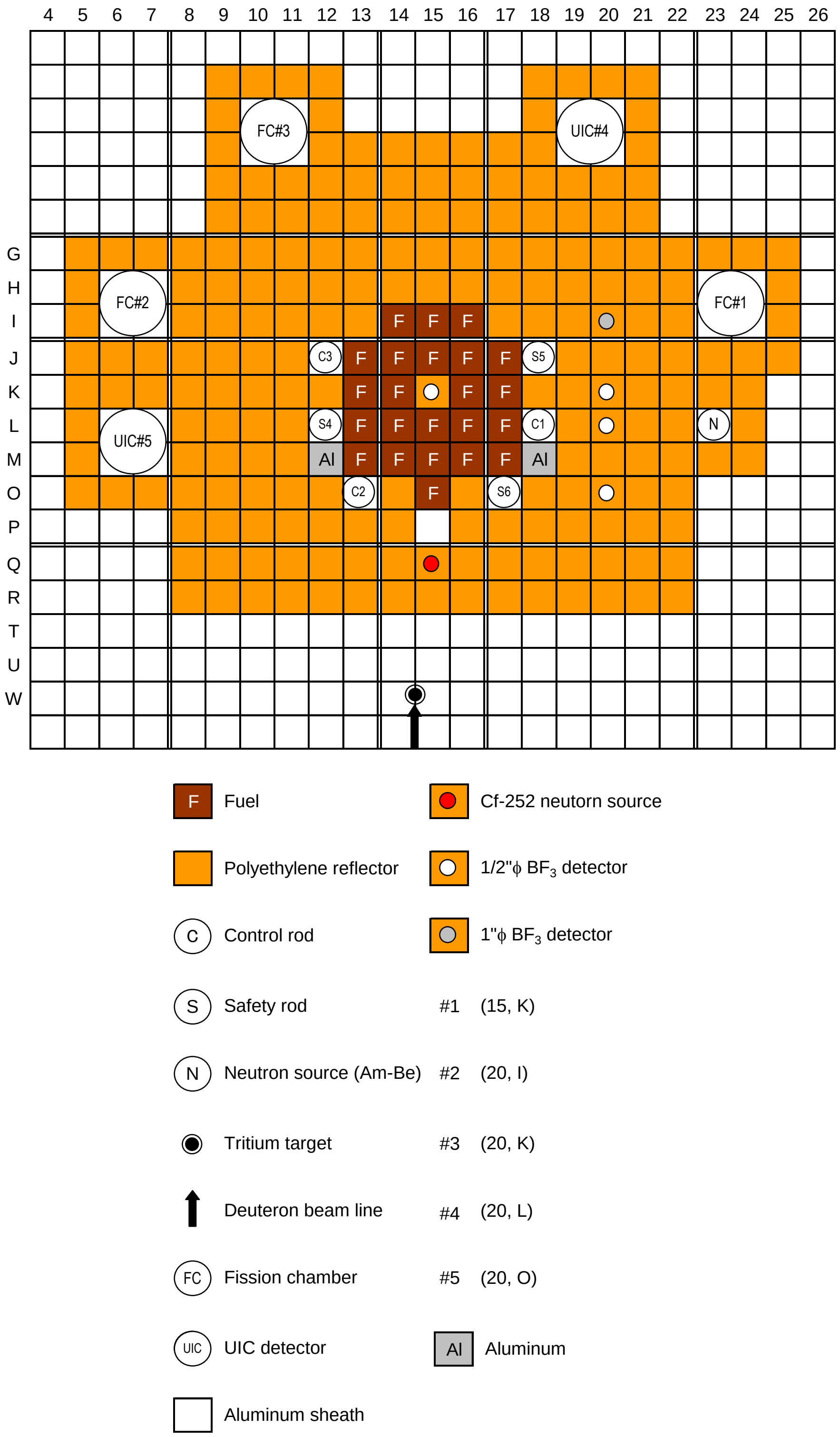

Fig. 6-1 Core configuration of subcriticality measurement using Source multiplication method (Cases II-1 through II-4)

6-2 Cases II-5 through II-7

Table VI-3 Control, safety rod and Cf-252 positions in subcriticality measurement

Case	C1	C2	C3	S4, S5, S6	Cf-252 source
II-5	0.0	0.0	0.0	0.0	(15, K)
II-6	0.0	0.0	0.0	0.0	(16, J)
II-7	0.0	0.0	0.0	0.0	(16, L)

Table VI-4 Measured subcriticality using source multiplication method at each detector Position shown in Fig. 6-2

Case	Reference (%Δk/k)	(10, L)	(10, J)	(10, H)	(15, E)	FC#1	FC#2	FC#3
II-5	1.64 (0.02)	1.75 (0.02)	1.50 (0.02)	1.59 (0.02)	1.30 (0.01)	1.76 (0.02)	1.67 (0.02)	1.58 (0.02)
II-6		1.96 (0.02)	1.83 (0.02)	1.59 (0.02)	1.49 (0.01)	1.71 (0.02)	1.68 (0.02)	1.57 (0.02)
II-7		1.93 (0.02)	1.85 (0.02)	1.61 (0.02)	1.54 (0.01)	1.76 (0.02)	1.70 (0.02)	1.59 (0.02)

( ): Error of subcriticality (%Δk/k)

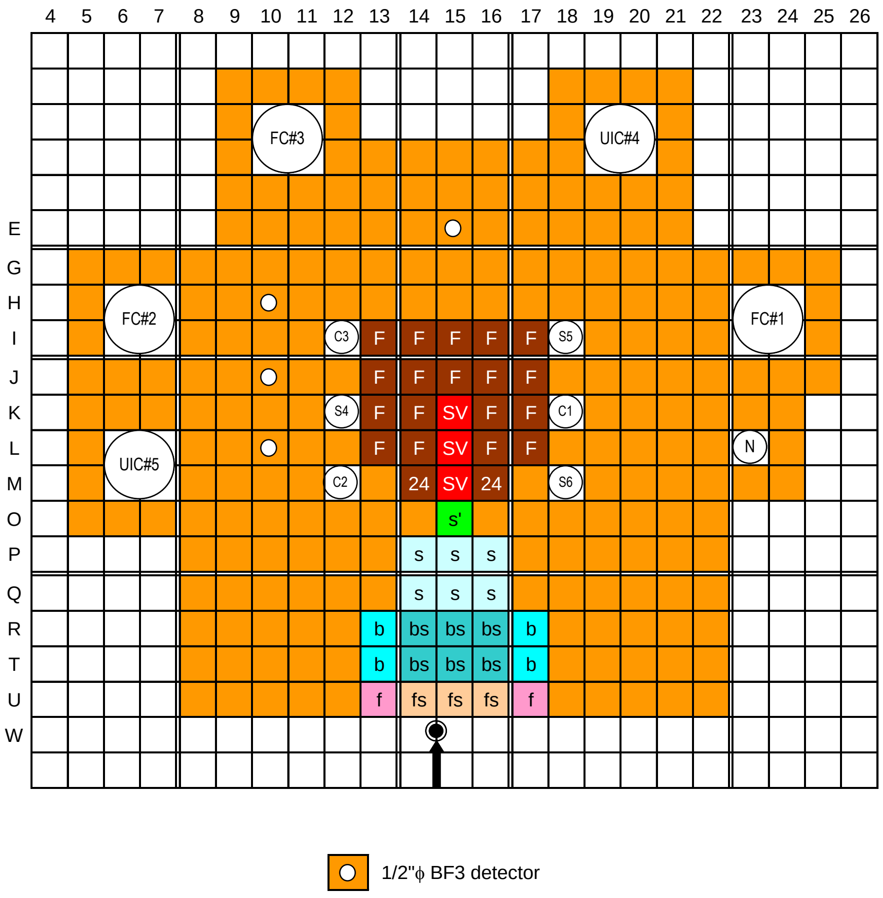

Fig. 6-2 Core configuration of subcriticality measurement using Source multiplication method (Cases II-5 through II-7)

6-3 Cases II-8 through II-10

Table VI-5 Control, safety rod and Cf-252 positions in subcriticality measurement

Case	C1	C2	C3	S4, S5, S6	Cf-252 source
II-8	0.0	0.0	0.0	1200.0	(15, K)
II-9	0.0	0.0	0.0	0.0	(16, J)
II-10	0.0	0.0	0.0	0.0	(16, L)

Table VI-6 Measured subcriticality using source multiplication method at each detector Position shown in Fig. 6-3

<table>
<tr><th>Case</th><th>Reference
(%Δk/k)</th><th>(10, L)</th><th>(10, J)</th><th>(10, H)</th><th>(15, E)</th><th>FC#1</th><th>FC#2</th><th>FC#3</th></tr>
<tr><td>II-8</td><td>7.64
(0.08)</td><td>10.2
(0.10)</td><td>11.3
(0.11)</td><td>13.5
(0.14)</td><td>2.98
(0.03)</td><td>—</td><td>—</td><td>—</td></tr>
<tr><td>II-9</td><td rowspan="2">8.57
(0.09)</td><td>23.3
(0.23)</td><td>22.0
(0.22)</td><td>20.8
(0.21)</td><td>3.12
(0.03)</td><td>—</td><td>—</td><td>—</td></tr>
<tr><td>II-10</td><td>12.9
(0.13)</td><td>8.67
(0.09)</td><td>15.5
(0.16)</td><td>3.10
(0.03)</td><td>—</td><td>—</td><td>—</td></tr>
</table>

( ): Error of subcriticality (%Δk/k)

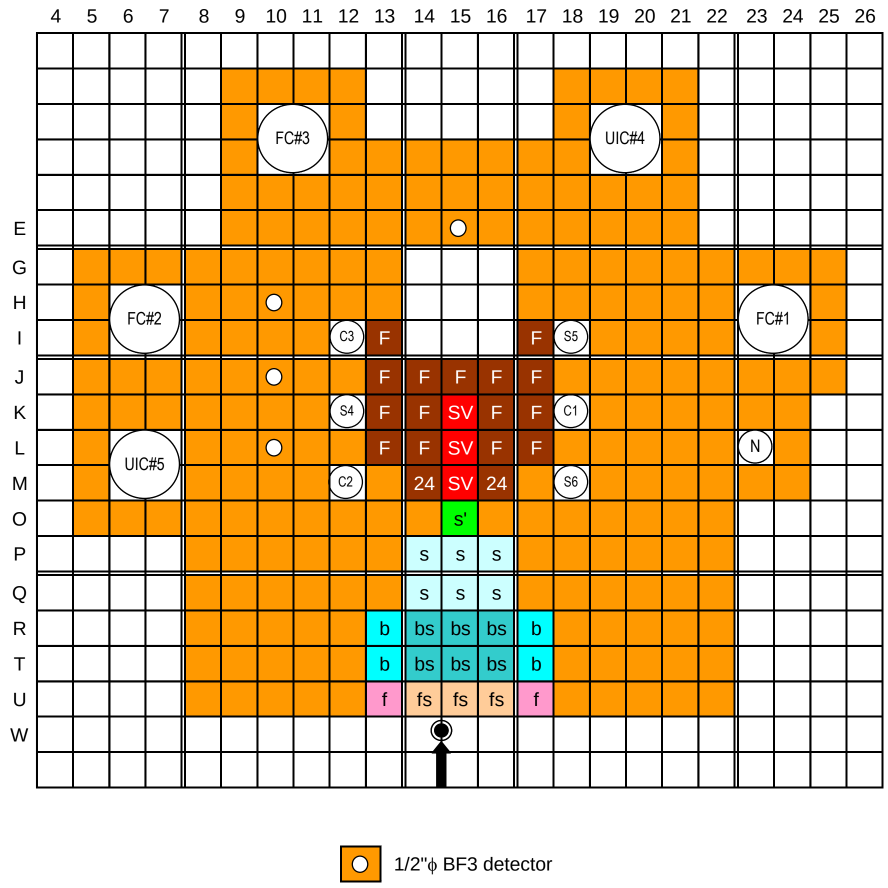

Fig. 6-3 Core configuration of subcriticality measurement using Source multiplication method (Cases II-8 through II-10)

7. Pulsed neutron method

Table VII-1 Control and safety rod positions in subcriticality system

Case name	C1	C2	C3	S4	S5	S6	Pulsed width (μs)	Pulsed period (ms)
III-1	0.0	0.0	0.0	1200.0	1200.0	1200.0	60	12
III-2	0.0	0.0	0.0	0.0	0.0	0.0	80	32
III-3	1200.0	1200.0	1200.0	1200.0	1200.0	1200.0	55	32
III-4	0.0	0.0	0.0	1200.0	1200.0	1200.0	20	16
III-5	0.0	0.0	0.0	0.0	0.0	0.0	30	12
III-6	1200.0	1200.0	1200.0	1200.0	1200.0	1200.0	30	12
III-7	0.0	0.0	0.0	1200.0	1200.0	1200.0	30	12
III-8	0.0	0.0	0.0	0.0	0.0	0.0	30	12
III-9	1200.0	1200.0	1200.0	1200.0	1200.0	1200.0	50	10

Table VII-2 Measured subcriticality using pulsed neutron method at each optical fiber detector position shown in Fig. 3-1

Case name	Fiber #1 (%Δk/k)	Fiber #2 (%Δk/k)	Fiber #3 (%Δk/k)
III-1	0.99±0.01	0.96±0.01	0.99±0.01
III-2	1.88±0.02	2.15±0.02	1.78±0.02
III-3	2.55±0.03	3.12±0.03	2.42±0.02
III-4	3.40±0.03	3.25±0.03	3.63±0.04
III-5	4.49±0.04	4.00±0.04	4.60±0.05
III-6	5.89±0.06	6.54±0.07	6.87±0.07
III-7	6.59±0.07	10.01±0.10	7.56±0.08
III-8	7.55±0.08	8.18±0.08	8.64±0.09
III-9	10.24±0.10	12.28±0.12	11.93±0.12

Table VII-3 Measured neutron decay constant using pulsed neutron method at each optical fiber detector position shown in Fig. 7-1

Case name	Fiber #1 (1/sec)	Fiber #2 (1/sec)	Fiber #3 (1/sec)
III-1	369±4	372±6	360±5
III-2	570±6	586±10	607±7
III-3	640±5	640±9	604±7
III-4	817±14	820±24	788±17
III-5	994±19	1034±34	922±23
III-6	1204±21	1202±37	1130±23
III-7	1419±30	1364±51	1510±41
III-8	1418±33	1560±64	1468±44
III-9	1640±21	1797±40	1701±24

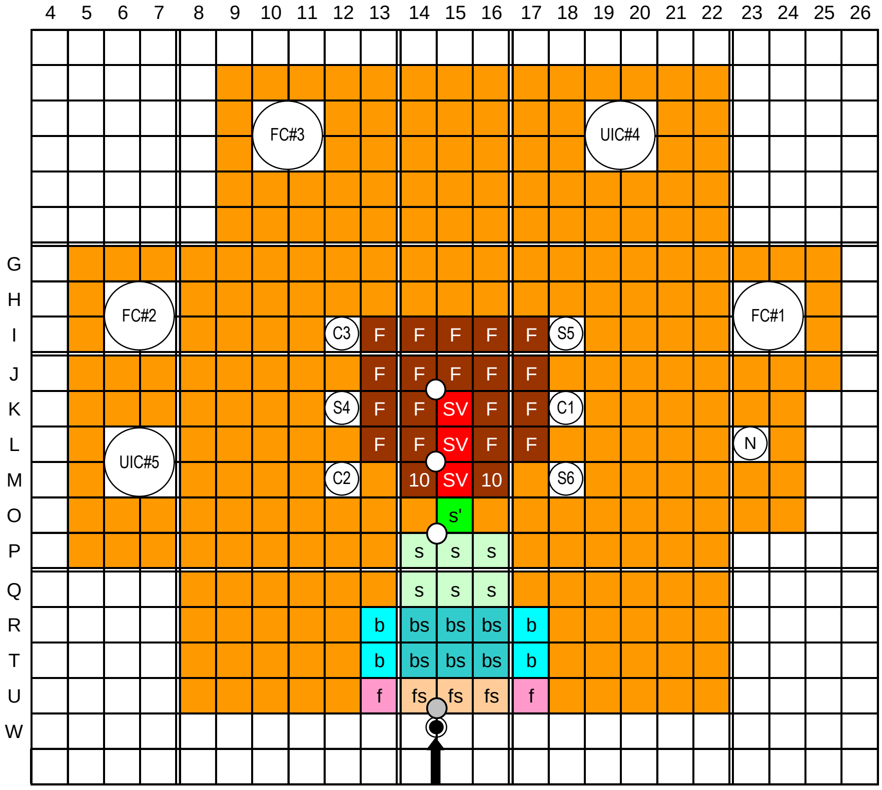

○ LiF optical fiber

● ThO_2 optical fiber

Fiber #1: (14-15, J-K)

Fiber #2: (14-15, L-M)

Fiber #3: (14-15, O-P)

Fig. 7-1 Core configuration of subcriticality measurement using pulsed neutron method (Cases III-1 through III-2)

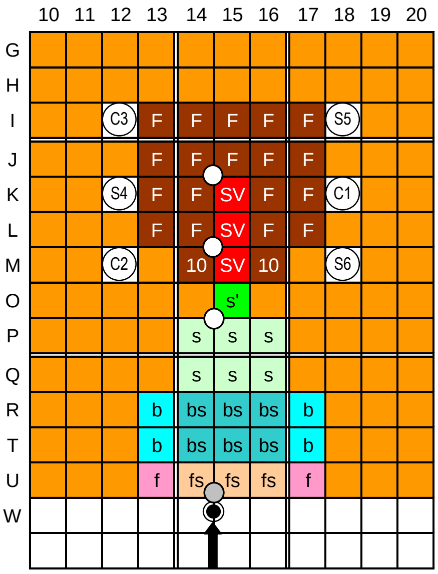

(a) Cases III-1 and III-2

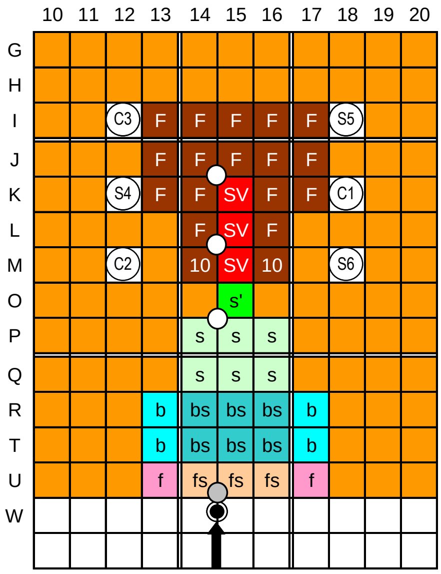

(b) Cases III-3 through III-5

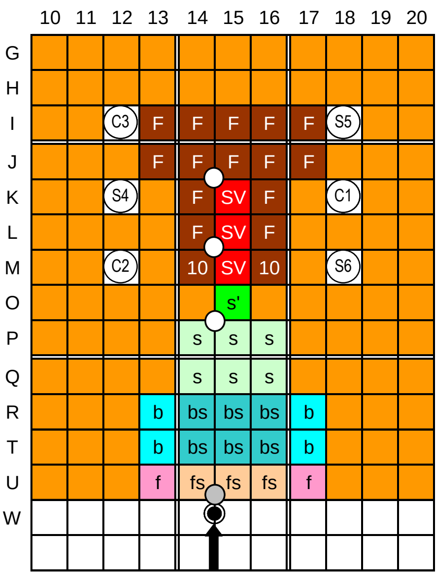

(c) Cases III-6 through III-8

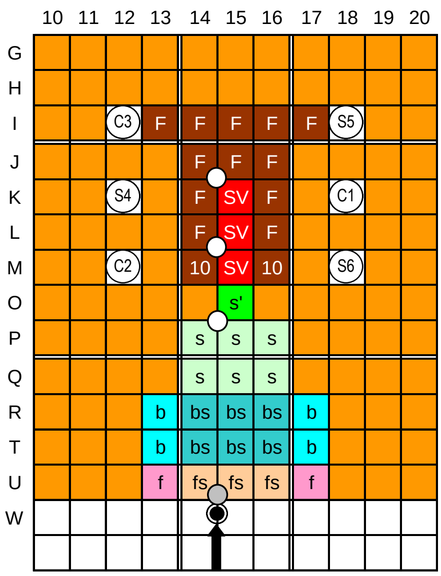

(d) Case III-9

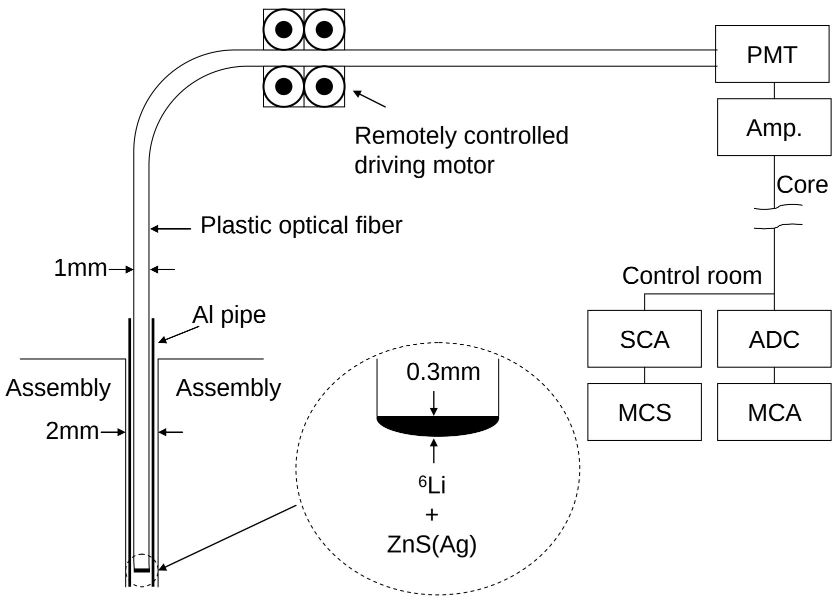

Fig. 7-2 Schema of an optical fiber detection system